

## Chapter 28 Problems: Electronic Spectroscopy

### 1. Why all the interest in diatomic molecules?

*Answer:* For diatomics and polyatomics, spectroscopic parameters are used to calculate thermodynamic equilibrium constants and kinetic rate constants. Reasons for all the fuss about diatomics include:

- (a). Diatomics play a direct role in many chemical reactions,  $O_2$  being a primary example. Atmospheric chemistry requires detailed knowledge of many diatomics including OH,  $O_2$ ,  $N_2$ , NO, CO,  $Cl_2$ ,  $Br_2$ ,  $I_2$ , ClO, BrO, HCl, and the corresponding ions. Diatomics act as ligands in metal complexes, including CO and NO.  $H_2$  is a commonly used reducing agent in the synthetic laboratory. CO blocks  $O_2$  transport in hemoglobin and is a major industrial reducing agent in metallurgical applications. The halogens are used as gas phase disinfection agents. Chemical vapor deposition of thin films involves diatomics, including  $H_2$  and  $F_2$ . Hydride epitaxial growth of thin films using HCl and  $H_2$  is used in the semiconductor industry. Industrial high power ultraviolet excimer lasers are based on stimulated emission from excited state diatomics, including ArF, XeBr, XeCl, XeF, and KrF. Combustion engineering is based on chemical kinetics of gas phase free radical species, many of which are diatomics or derived from reactions with neutral diatomics, such as CO,  $N_2$ ,  $C_2$ , and  $O_2$ .
- (b). Our basic understanding of bonding, through bond strength measures, is based on diatomics. The correlations displayed in Figure 26.4.12 are central in this regard. For example, bond strength increases with increasing bond order and as bond strength increases equilibrium bond length decreases. These fundamental relationships are based on dissociation energies, force constants, and bond lengths that result from spectroscopic studies of diatomics.
- (c). To a first level of approximation, chemical bonding is a pairwise interaction. Knowing the coarseness of the approximation, we often think of chemical bond strength as being a function of just the two atoms involved in each bond. For example, bond enthalpy tables are based on atom pairs, Table 8.8.1. Pauling electronegativities are based on diatomic bond dissociation energies. Eq. 26.3.13. Of course bonding is extensively delocalized, but pair-wise interactions are still an important viewpoint. In this regard, diatomics are the fundamental reference point for pair-wise bonding interactions.<sup>1</sup>
- (d). Diatomics are a good point of reference. When we determine the bonding in a complicated molecule, diatomics provide a useful comparison that allows us to identify unusual bonding interactions. These comparisons are often based on bond strength correlations and changes in effective electronegativity as previewed in part (c).
- (e). Diatomics are useful for validating electronic structure methods. If an electronic structure method can't reproduce bond dissociation energies for diatomics, then there is little hope of accurately predicting the properties of polyatomics. Excited electronic states are a particular challenge for electronic structure calculations. "Ground-truthing" with data from diatomics is necessary to help develop new excited state methods.
- (f). Diatomics often have resolved rotational and vibrational fine-structure, while polyatomics often do not. Rotational fine-structure is necessary for the determination of bond lengths in excited state species. Vibrational fine-structure is necessary for determination of the shape of potential energy surfaces.
- (g). Non-adiabatic kinetic processes are difficult to model, so keeping things simple by studying reactions of diatomics is often necessary.

2. Calculate the transition wave number for the ground electronic state to first excited singlet state transition in carbon monoxide. Assume the ground state vibrational-rotational and quantum numbers are  $\nu'' = 0, J'' = 3$  and the excited state quantum numbers are  $\nu' = 3, J' = 4$ . The spectroscopic constants are given below.<sup>2,3</sup>

State	$\tilde{T}_e$ (cm <sup>-1</sup> )	$\tilde{\nu}_e$ (cm <sup>-1</sup> )	$\chi_e \tilde{\nu}_e$ (cm <sup>-1</sup> )	$\tilde{B}_e$ (cm <sup>-1</sup> )	$\tilde{\alpha}_e$ (cm <sup>-1</sup> )	$\tilde{D}_e$ (cm <sup>-1</sup> )
A <sup>1</sup> Π	65075.7	1518.2	19.4	1.6115	0.02325	7.33x10 <sup>-6</sup>
X <sup>1</sup> Σ <sup>+</sup>	0	2169.814	13.288	1.93128	0.017504	6.12x10 <sup>-6</sup>

*Answer:* The plan is to use Eqs. 27.6.5 and 28.1.3.

With Eq. 27.6.5, the rotational constant for the ground electronic state with  $\nu = 0$  is:

$$\tilde{B}_0^{\text{gs}} = \tilde{B}_e^{\text{gs}} - \tilde{\alpha}_e^{\text{gs}} (\nu + \frac{1}{2}) = 1.93128 \text{ cm}^{-1} - 0.017504 \text{ cm}^{-1} (0 + \frac{1}{2}) = 1.92253 \text{ cm}^{-1}$$

For the excited electronic state with  $\nu = 3$  the rotational constant is:

$$\tilde{B}_\nu^{\text{ex}} = \tilde{B}_e^{\text{ex}} - \tilde{\alpha}_e^{\text{ex}} (\nu + \frac{1}{2}) = 1.6115 \text{ cm}^{-1} - 0.02325 \text{ cm}^{-1} (3 + \frac{1}{2}) = 1.53013 \text{ cm}^{-1}$$

With Eq. 28.1.3, the energy of the ground state for  $\nu'' = 0, J'' = 3$  is:

$$\begin{aligned} \tilde{E}_{i,\nu,J} &= \tilde{T}_{e,i} + \tilde{\nu}_{e,i} (\nu + \frac{1}{2}) - \chi_{e,i} \tilde{\nu}_{e,i} (\nu + \frac{1}{2})^2 + \tilde{B}_{\nu,i} J(J+1) - \tilde{D}_{e,i} [J(J+1)]^2 \\ \tilde{E}_{\text{gs},0,3} &= \tilde{T}_e^{\text{gs}} + \tilde{\nu}_e^{\text{gs}} (0 + \frac{1}{2}) - \chi_e^{\text{gs}} \tilde{\nu}_e^{\text{gs}} (0 + \frac{1}{2})^2 + \tilde{B}_0^{\text{gs}} 3(3+1) - \tilde{D}_e [3(3+1)]^2 \\ &= 0 + 2169.814(0 + \frac{1}{2}) - 13.288(0 + \frac{1}{2})^2 + 1.92253[3(3+1)] - 6.12 \times 10^{-6} [3(3+1)]^2 \\ &= 1104.65 \text{ cm}^{-1} \end{aligned}$$

The excited state energy for  $\nu' = 3, J' = 4$  is:

$$\begin{aligned} \tilde{E}_{\text{gs},0,3} &= \tilde{T}_e^{\text{ex}} + \tilde{\nu}_e^{\text{ex}} (0 + \frac{1}{2}) - \chi_e^{\text{ex}} \tilde{\nu}_e^{\text{ex}} (0 + \frac{1}{2})^2 + \tilde{B}_0^{\text{ex}} 3(3+1) - \tilde{D}_e^{\text{ex}} [3(3+1)]^2 \\ &= 65075.7 + 1518.2 (0 + \frac{1}{2}) - 19.4 (0 + \frac{1}{2})^2 + 1.5301[3(3+1)] - 7.33 \times 10^{-6} [3(3+1)]^2 \\ &= 70182.35 \text{ cm}^{-1} \end{aligned}$$

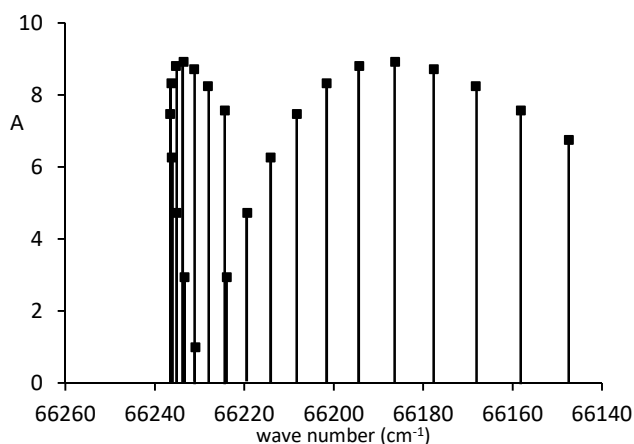
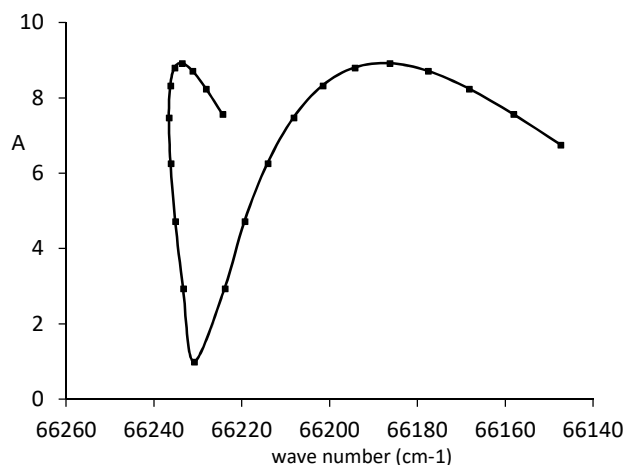
The transition wave number is given by the difference:  $\tilde{\nu} = 69077.70 \text{ cm}^{-1}$ .

3. In rotation-vibration absorption, with  $\tilde{B}' < \tilde{B}''$ , each line moves to lower wave number in proportion to the  $J''^2$  value, Eqs. 27.6.8-27.6.9. The R-branch lines get closer together and the P-branch lines get further apart. Please review Problem 27.30. In electronic absorption, the rotational constant in the upper electronic states often differs markedly from the ground electronic state. Write a spreadsheet to simulate the electronic absorption spectrum of carbon monoxide for the  $\nu'' = 0$  to  $\nu' = 1$  vibrational transition. The spectroscopic constants are listed in the previous problem. Neglect centrifugal distortion. [Hints: Refer to the hint for Problem 27.30, however this time your plot will be clearer if you choose a scatter plot with marker symbols and a connecting line. Include transitions for  $J'' = 0$  to 10 for the R- and P-branches. To start with, to make the plot clearer you may want to use  $\tilde{B}_e = 1.93128 \text{ cm}^{-1}$  for both electronic states. Then switch to  $\tilde{B}_e = 1.6115 \text{ cm}^{-1}$  for the excited state.]

*Answer:* The plan is to modify the spreadsheet for Problem 27.30 to calculate the  $\tilde{B}_v$  value for the ground and excited electronic state and specific vibrational quantum numbers  $v'' = 0$  to  $v' = 1$ . The previous problem discusses the necessary calculations.

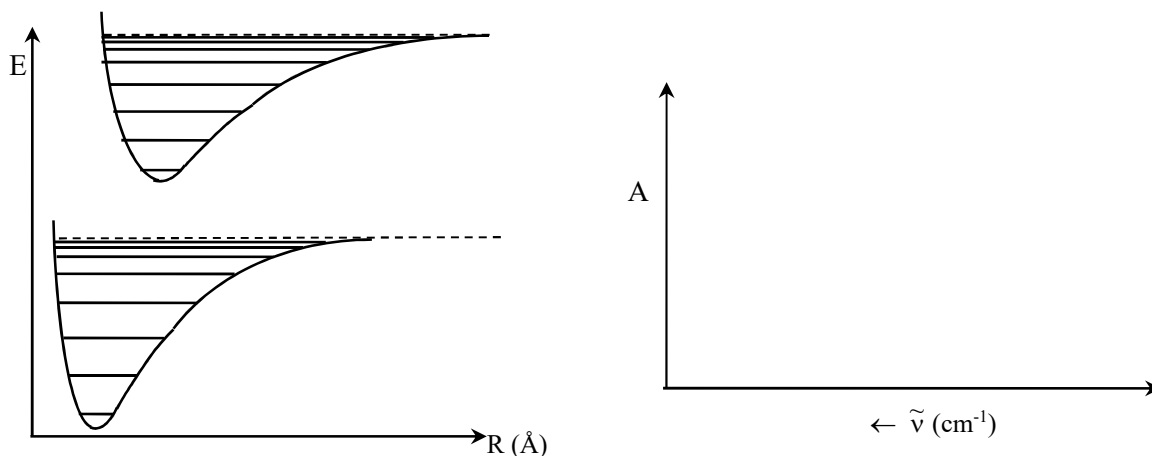
Using the data and calculations from the previous problem, the spreadsheet appears as follows. The number of rows were increased to plot a wider range of transitions, from  $J'' = 0$  to 10 for the R- and P-branches. The “stick” spectrum is also shown for this problem. The R-branch lines move far enough to lower wave number that the transitions for high  $J''$  decrease in wave number even though  $J''$  is increasing. The rotational fine-structure lines “fall back” on each other. This effect is common in electronic spectroscopy.

A					
1					
2	$T_e$	0	65075.7	$\text{cm}^{-1}$	
3	$V_e$	2169.81	1518.2	$\text{cm}^{-1}$	
4	$\chi_{eVe}$	13.288	19.4	$\text{cm}^{-1}$	
5	$v$	0	1		
6	$v_v$	1081.58	2233.65	$\text{cm}^{-1}$	
7	$B_e$	1.93128	1.6115	$\text{cm}^{-1}$	
8	$\alpha_e$	0.01750	0.02325	$\text{cm}^{-1}$	
9	$B_v$	1.92253	1.576625	$\text{cm}^{-1}$	
10					
11	$J''$	$J'$	$F(J'')$ ( $\text{cm}^{-1}$ )	$\nu$ ( $\text{cm}^{-1}$ )	$p(J'')$
12	10	11	-3.36358	66224.401	7.568
13	9	10	0.40123	66228.166	8.243
14	8	9	3.474234	66231.239	8.716
15	7	8	5.855432	66233.620	8.921
16	6	7	7.544824	66235.310	8.804
17	5	6	8.54241	66236.307	8.327
18	4	5	8.84819	66236.613	7.476
19	3	4	8.462164	66236.227	6.262
20	2	3	7.384332	66235.149	4.729
21	1	2	5.614694	66233.380	2.945
22	0	1	3.15325	66230.918	1.000
23	1	0	-3.84506	66223.920	2.945
24	2	1	-8.38192	66219.383	4.729
25	3	2	-13.6106	66214.154	6.262
26	4	3	-19.5311	66208.234	7.476
27	5	4	-26.1433	66201.622	8.327
28	6	5	-33.4474	66194.318	8.804
29	7	6	-41.4433	66186.322	8.921
30	8	7	-50.131	66177.634	8.716
31	9	8	-59.5105	66168.255	8.243
32	10	9	-69.5818	66158.183	7.568
33	11	10	-80.3449	66147.420	6.758



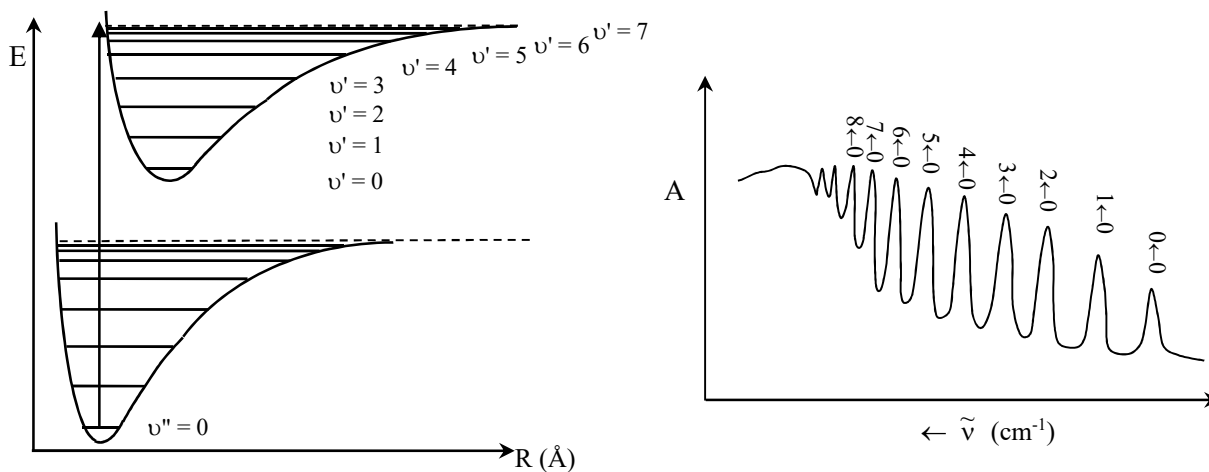
The maximum wave number is called the **band head**. The  $0 \leftarrow 0$  transition is called the **band origin**. In this problem the band origin is obscured, because of the extensive overlap of the R- and P-branches.

4. Predict the intensities of the different vibrational transitions in the electronic absorption spectrum of the following system. Show at least four peaks. Label each transition in the energy level diagram with the vibrational quantum numbers for the transition and each corresponding peak in the spectrum (e.g.  $4 \leftarrow 0$ ).



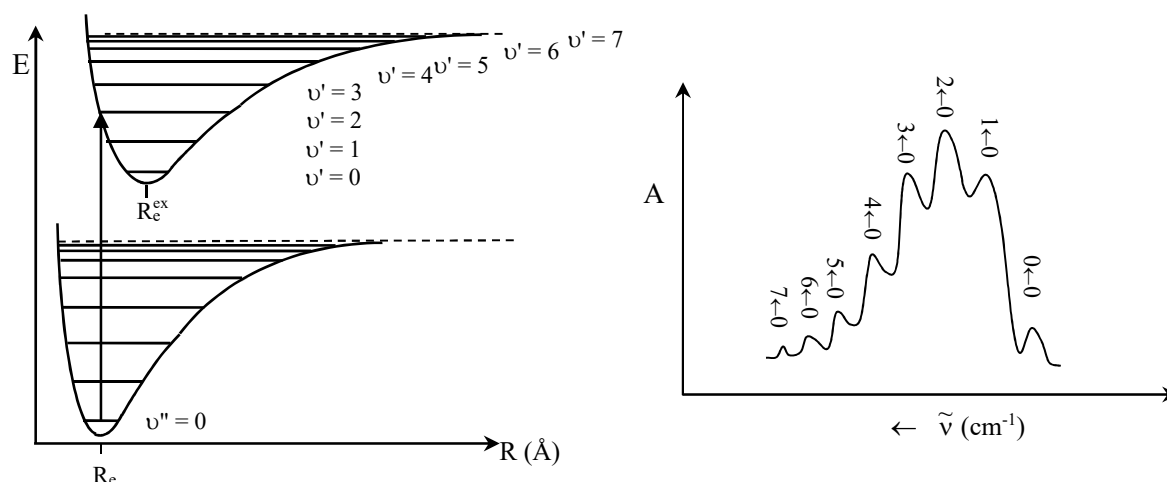
*Answer:* The plan is to draw in the vertical transition to predict the vibrational fine-structure transition with the largest Franck-Condon factor.

The vertical transition intersects the excited state potential energy curve above the dissociation limit. The highest intensity transitions are to vibrational levels near the convergence limit and to the translational continuum. The peak spacing goes to zero at the convergence limit



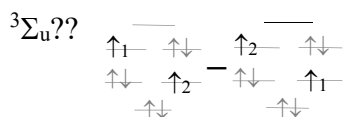
5. Show the relationship between the ground state and excited state potential energy curves for an electronic transition that has a maximum probability for the  $2 \leftarrow 0$  vibrational fine-structure transition. Draw the corresponding absorption spectrum. Label each transition in the energy level diagram with the vibrational quantum numbers for the transition and each corresponding peak in the spectrum (e.g.  $4 \leftarrow 0$ ). (Use the potential energy curves shown in the previous question for the style of your sketch).

*Answer:* The plan is to position the equilibrium internuclear separations of the ground and excited state potential energy curves to give the vertical transition with  $2 \leftarrow 0$  as the largest Franck-Condon factor.

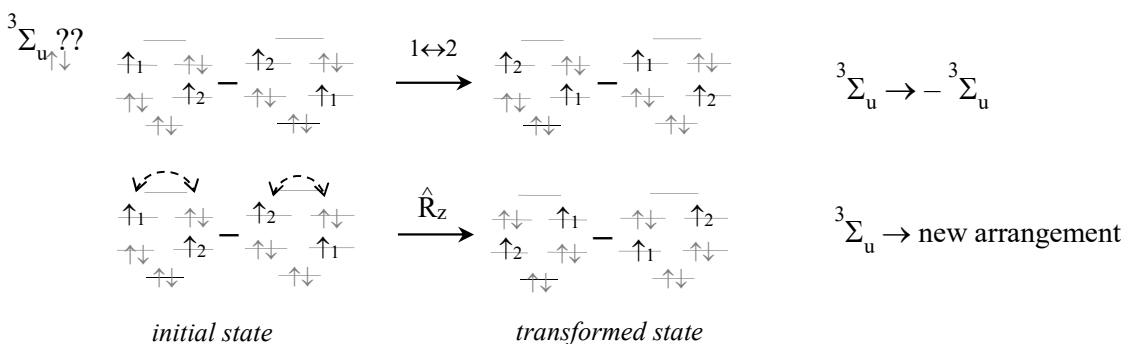


Intense excitations into low lying vibrational levels of the excited state correspond to small changes in equilibrium internuclear separation, as shown in the figure above. Transitions of other adjacent vibrational levels typically have comparable intensities. The vertical transition just predicts the most intense. The absorption spectrum resembles that for benzene, Figure 28.1.12.

6. (a). In Figure 28.1.9b we needed to take the linear combination of four specific assignments to generate a state that satisfies both the Pauli Exclusion Principle and reflection symmetry. Why four states instead of two? Show that the following state does not properly account for electron indistinguishability and reflection symmetry:



*Answer:* Consider transformation of the state with respect to exchange of spin labels and reflection:

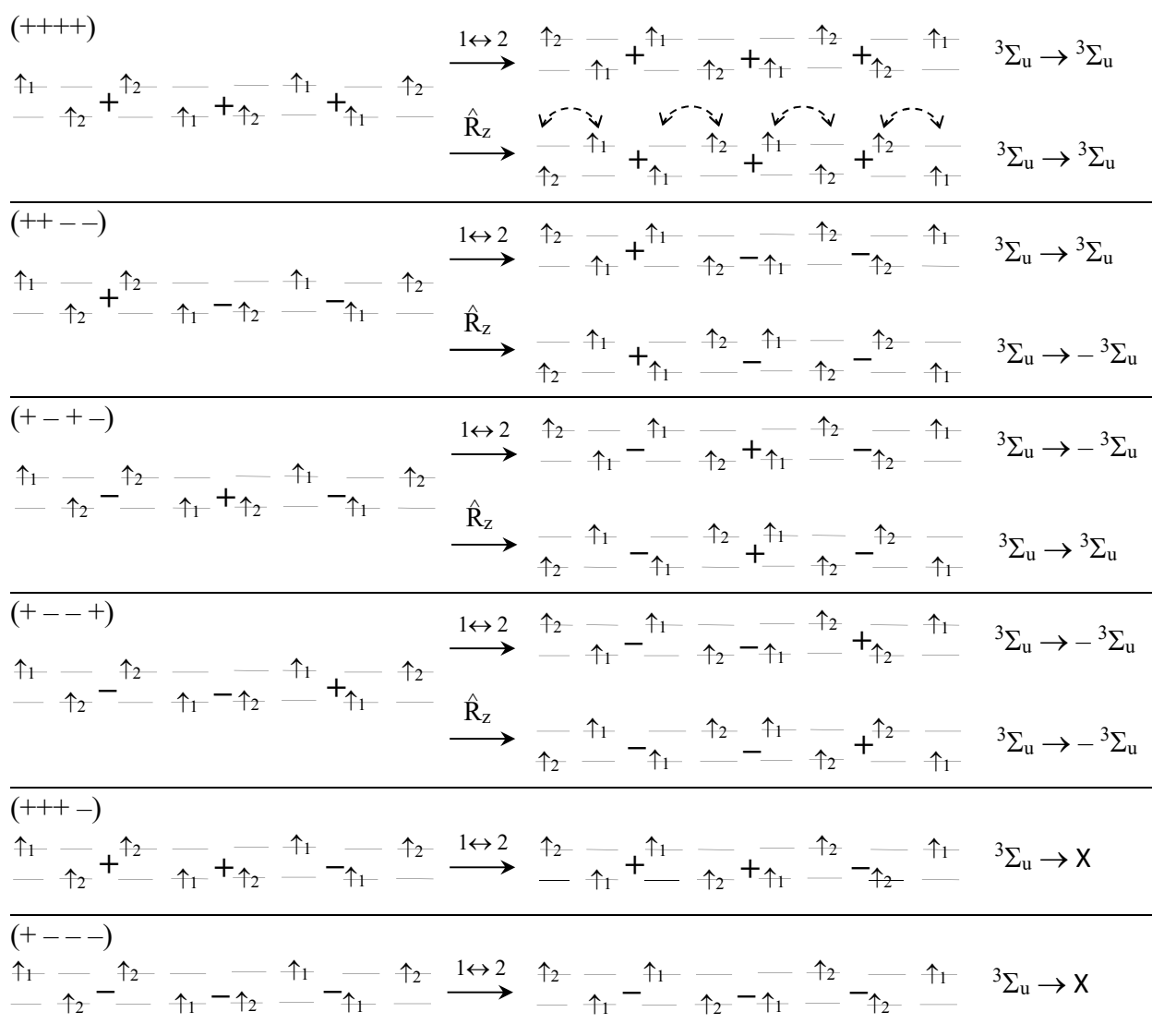


The given linear combination is anti-symmetric with respect to exchange of spin labels, as required for the spatial part of a triplet state, but reflection symmetry results in a different set of singly occupied orbitals than the initial state. This linear combination is neither symmetric nor anti-symmetric with respect to reflection, it transforms to give a different state. The linear

combinations that transform as symmetric or anti-symmetric with respect to exchange of spin labels and reflection are given in Figure 28.1.9.

7. In Figure 28.1.10 we needed to take the linear combination of four specific assignments to generate a state that satisfies both the Pauli Exclusion Principle and reflection symmetry. However, there are eight possible combinations of the coefficients that give equal weight to each assignment:  $(++++)$ ,  $(++--)$ ,  $(+-+-)$ ,  $(+--+)$ ,  $(+++ -)$ ,  $(+---)$ ,  $(+ -++)$ ,  $(+ -+-)$ . Show that only the two linear combinations listed in Figure 28.1.10 properly account for electron indistinguishability and reflection symmetry for the  $\Sigma_u$  triplet terms and two more for the singlet terms.

*Answer:* To make the states easier to compare, show only the singly occupied states. Then determine the symmetry with respect to exchange of spin labels and reflection:



Similarly (+ - ++) and (++) - +) don't transform to give either the original state or its negative. Summarizing, the eight possible states give two states that are anti-symmetric with respect to exchange of spin labels and are either symmetric or anti-symmetric with respect to reflection. These states have the spatial symmetry appropriate to match the symmetric spin parts of the triplet terms. In addition there are two states that are symmetric with respect to exchange of spin labels and are either symmetric or anti-symmetric with respect to reflection. This second pair has the spatial symmetry appropriate to match the anti-symmetric spin part of the singlet terms:

Linear combination	Label exchange	Reflection	Term
(++++)	+	+	$^1\Sigma_u^+$
(++--)	+	-	$^1\Sigma_u^-$
(+-+-)	-	+	$^3\Sigma_u^+$
(+---)	-	-	$^3\Sigma_u^-$
(+++ -)	X		
(+----)	X		
(+ - ++)	X		
(++ - +)	X		

8. In Chapter 25, we determined the complete set of atomic terms for a given electronic configuration by exhaustively enumerating all the possible explicit orbital assignments. In this chapter we took a bit of a short-cut. However, it is still informative to determine all possible molecular terms by exhaustive enumeration. Luckily, diatomic electronic states are simpler, because the  $\pi$  levels are only doubly degenerate. For example, the  $p^1$  atomic configuration gives a  $^2P$  term with  $M_L = \{1, 0, -1\}$ . However, the  $(\sigma_{g,2pz})^2 (\pi_{u,2p})^1$  molecular configuration corresponds to only  $M_\lambda = \{1, -1\}$ , because there are only two degenerate  $\pi$ -molecular orbitals:

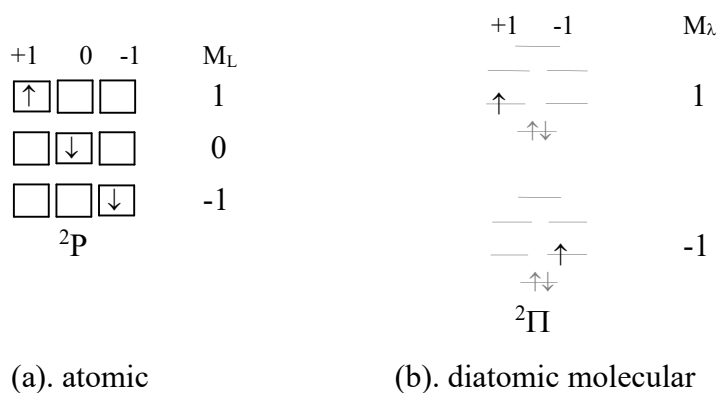


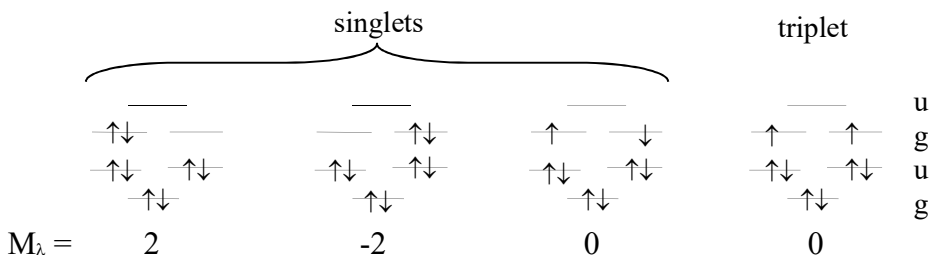
Figure P28.8.1: (a). The  $p^1$  atomic configuration is triply degenerate with  $M_L = \{1, 0, -1\}$ . (b). The  $(\sigma_{g,2pz})^2 (\pi_{u,2p})^1$  molecular configuration corresponds to only  $M_\lambda = \{1, -1\}$ , since the  $\pi$  orbitals are doubly degenerate.

Similarly, a  $\Delta$  term is also doubly degenerate,  $M_\lambda = \{2, -2\}$ . Show that the molecular terms for the configuration  $KK (\sigma_{g,2s})^2 (\sigma_{u,2s}^*)^2 (\sigma_{g,2pz})^2 (\pi_{u,2p})^4 (\pi_{g,2p}^*)^2$  are  $^3\Sigma_g + ^1\Delta_g + ^1\Sigma_g$ , by exhaustive

enumeration of explicit molecular orbital assignments. Include the parity, g or u (you don't need to find the reflection symmetry).

*Answer:* The explicit orbital assignments are:

$$KK (\sigma_{g,2s})^2 (\sigma_{u,2s}^*)^2 (\sigma_{g,2pz})^2 (\pi_{u,2p})^4 (\pi_{g,2p}^*)^2$$



Using the same procedure that we used for atomic term symbols, we first list all the  $M_\lambda$  values for the singlet states:

$$M_\lambda = \{2, 0, -2\}$$

With  $\Lambda = 2$ , the first term is a  ${}^1\Delta$  term. Removing  $M_\lambda = \{2, -2\}$  leaves:

$$M_\lambda = \{0\}$$

The final singlet term is  ${}^1\Sigma$ . The only triplet gives  $\Lambda = 0$  for a  ${}^3\Sigma$  term. The parity of all the states is gguuuugg = g. The final terms are  ${}^1\Delta_g + {}^1\Sigma_g + {}^3\Sigma_g$ , in agreement with Figure 28.1.5a.

You may wonder why we don't consider assignments like the two below as distinct:



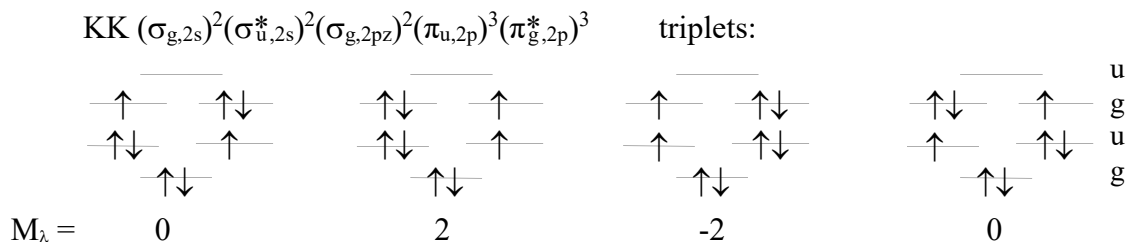
The assignment on the right is the same triplet assignment as on the left with all the spins flipped. Therefore, right-hand assignment doesn't represent a unique explicit orbital assignment. Instead, the two assignments are components of the same triplet state, with spin states  $\{\alpha\alpha, \alpha\beta + \beta\alpha, \beta\beta\}$ . For another example, the two states below are the same explicit assignment with all the spins flipped. So they aren't unique:



These two assignments are degenerate and combine in symmetry adapted linear combination to form the final  ${}^1\Sigma_g^+$  state, as shown in Figure 28.1.9b. In general, two states that are related by flipping all the spins are not unique for the purposes of determining the possible values of  $M_L$  for atoms or  $M_\lambda$  for molecules.

9. Find the molecular terms for the configuration  $KK (\sigma_{g,2s})^2(\sigma_{u,2s}^*)^2(\sigma_{g,2pz})^2(\pi_{u,2p})^3(\pi_{g,2p}^*)^3$  by exhaustive enumeration of explicit molecular orbital assignments. Include the parity, g or u (you don't need to find the reflection symmetry).

*Answer:* There are two degenerate  $\pi_{u,2p}$  orbitals for placement of one unpaired electron and two degenerate  $\pi_{g,2p}^*$  orbitals for placement of the second unpaired electron, so we expect  $2 \cdot 2 = 4$  explicit orbital assignments for triplet states and another 4 for singlet states. The explicit orbital assignments for the triplet states are:



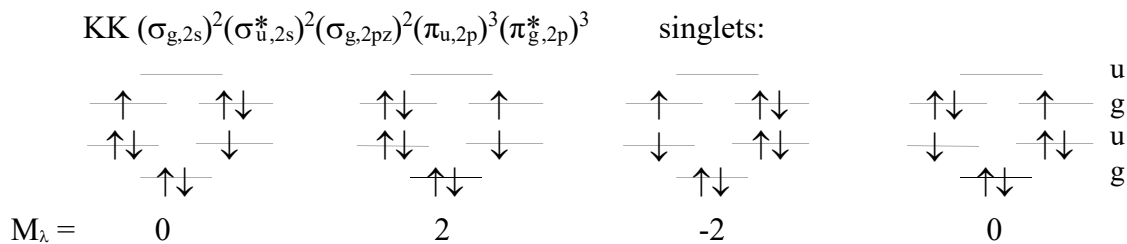
Using the same procedure that we used for atomic term symbols, we first list all the  $M_\lambda$  values for the triplet states:

$$M_\lambda = \{2, 0, 0, -2\}$$

With  $\Lambda = 2$ , the first term is a  ${}^3\Delta$  term. Removing  $M_\lambda = \{2, -2\}$  leaves:

$$M_\lambda = \{0, 0\}$$

The remaining terms are two  ${}^3\Sigma$  terms. The parity of all the states is  $gguuuggg = u$ . The singlet states are obtained by flipping one of the unpaired spins in the previous set:



The resulting  $M_\lambda$  set is the same as for the triplet states and the parity also remains the same. The final terms are  ${}^3\Delta_u + {}^3\Sigma_u + {}^3\Sigma_u$  and  ${}^1\Delta_u + {}^1\Sigma_u + {}^1\Sigma_u$  in agreement with Figure 28.1.5b. The repeat  ${}^3\Sigma$  and  ${}^1\Sigma$  terms show the necessity of considering the reflection symmetry.

10. For a homonuclear diatomic molecule, determine which of the following transitions is allowed or forbidden, assuming weakly coupled spin and orbital angular momenta.<sup>4</sup> [Note: identical term symbols can result from two different configurations; term symbols are unique within a given configuration.]



*Answer:* The plan is to note the selection rules, Eq. 28.1.12, for weakly coupled spin and orbital angular momenta.

The allowed transitions are  ${}^2\Sigma_g^- \leftarrow {}^2\Pi_u$ ,  ${}^1\Delta_g \leftarrow {}^1\Pi_u$ , and  ${}^3\Sigma_u^- \leftarrow {}^3\Sigma_g^-$  (the Schumann-Runge band is  ${}^3\Sigma_u^- \leftarrow {}^3\Sigma_g^-$ ). The forbidden terms and the offended selection rule are:

Transition	Rule broken
${}^1\Sigma_g^- \leftarrow {}^1\Sigma_g^-$	$g \rightarrow u$ or $u \rightarrow g$
${}^1\Delta_u \leftarrow {}^1\Sigma_g^+$	$\Delta\Lambda = 0, \pm 1$
${}^1\Sigma_g^- \leftarrow {}^3\Sigma_u^-$	$\Delta S = 0$

11. (a). Determine the possible values of the projection of the total angular momentum,  $\Omega = |\Lambda + \Sigma_s|$ , for a  ${}^3\Delta$  term. (b). Determine if the transition to each of these  ${}^3\Delta$  terms from a  ${}^3\Pi_0$  state is allowed or forbidden.

*Answer:* The plan is to note that the projection of the spin angular momentum along the internuclear axis is from  $-S$  to  $+S$  in integer steps.<sup>4</sup>

For a  $\Delta$ -state,  $\Lambda = 2$ . For a triplet state,  $S = 1$  and then the projections are  $\Sigma_s = -1, 0, +1$ . The possible projection of the total angular momentum are then:

$$\Omega = |\Lambda + \Sigma_s| = 2 - 1, 2 + 0, 2 + 1 = 1, 2, 3 \quad \text{giving } {}^3\Delta_1, {}^3\Delta_2, \text{ and } {}^3\Delta_3 \text{ terms}$$

The selection rules,  $\Delta\Lambda = 0, \pm 1$ ;  $\Delta S = 0$ ; and  $\Delta\Omega = 0, \pm 1$  give:

$$\text{Allowed: } {}^3\Delta_1 \leftarrow {}^3\Pi_0$$

$$\text{Forbidden: } {}^3\Delta_2 \leftarrow {}^3\Pi_0, {}^3\Delta_3 \leftarrow {}^3\Pi_0 \quad (\Delta\Omega \text{ too large})$$

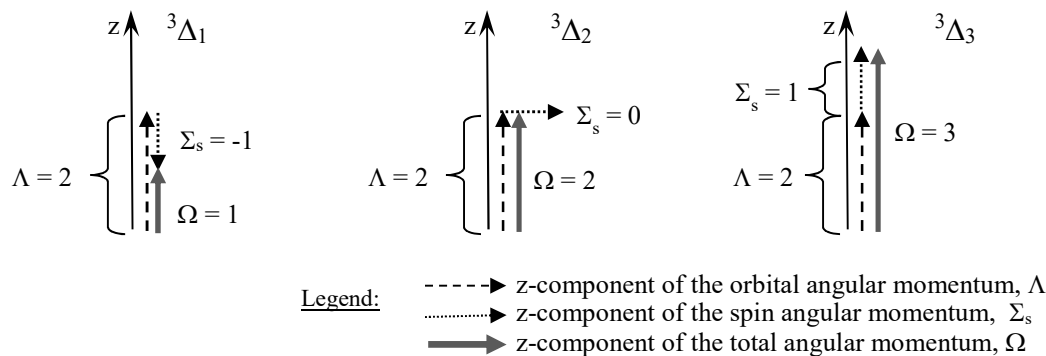
The  $\Delta\Omega = 0, \pm 1$  selection rule holds even in cases with strong spin-orbital coupling, when the  $\Delta\Lambda = 0, \pm 1$  and  $\Delta S = 0$  selections rules no longer apply.

Note: Most authors use the symbol  $\Sigma$  and not  $\Sigma_s$  for the projection of the spin angular momentum. Unfortunately then, the two uses of the symbol  $\Sigma$ , which are the term symbol and the projection of the spin, must be distinguished by context.

12. In Problem 25.31 we illustrated an angular momentum component diagram to help explain the occurrence of multiple total angular momentum states, given the projections of the orbital and spin angular momenta. Give the corresponding molecular diagram showing that the projections of the total angular momentum resolve  ${}^3\Delta$  terms into three states:  ${}^3\Delta_1$ ,  ${}^3\Delta_2$ , and  ${}^3\Delta_3$ . [Hint: simply replace  $M_L$ ,  $M_S$ , and  $M_J$  with  $\Lambda$ ,  $\Sigma_s$ , and  $\Omega$ . Note that  $\Lambda$  is always positive.<sup>4</sup> Use the  $S$  and  $\Lambda$  values corresponding to a  ${}^3\Delta$  term.]

*Answer:* The plan is to follow the diagram given in Problem 25.31, noting that  $\Lambda = 2$  and  $S = 1$ .

See the previous problem for the derivation of the three total angular momentum states. The diagrams are:



13. Describe in words the purpose of the Birge-Sponer extrapolation in the analysis of electronic absorption spectra.

*Answer:* The dissociation energy of the ground state is given by the wave number at the convergence limit as:

$$\tilde{D}_0 = \tilde{\nu}_{\infty 0} - \Delta \tilde{E}_{\text{atomic}} \quad (28.2.6)$$

This equation is not necessarily dependent on the Birge-Sponer extrapolation. If the convergence limit is obvious from the spectrum, the Birge-Sponer extrapolation is not necessary. Such cases include ClF, IBr, and ICl.<sup>5</sup> The purpose of the Birge-Sponer extrapolation is to determine the dissociation limit if the limit is obscured by noise or if vibrational fine-structure transitions near the dissociation limit are not observed.

Hertha Sponer (1895-1968) was a German physicist and physical chemist. The Birge-Sponer extrapolation was developed when she was on a Rockefeller Foundation fellowship with R. T. Birge at the University of California at Berkeley in 1925. In 1934, she was forced from her faculty position at the University of Göttingen by the Nazis, because she was a woman. In 1936 she was appointed as the first woman on the physics faculty at Duke University, where she remained active until 1966.

14. Describe in words the meaning and purpose of the Franck-Condon factors in the interpretation of electronic absorption spectra.

*Answer:* Franck-Condon factors determine the intensity of vibrational fine-structure transitions in absorption and emission spectroscopy as well as the rate of non-radiative energy transfer in internal conversion, intersystem crossing, and intermolecular energy transfer. Franck-Condon factors are given by the square of the overlap integral of the vibrational wave functions of the two coupled states. Franck-Condon integrals have a significant value only if the two vibrational wave functions have high probability at a common internuclear separation.

For absorption and emission spectra, we often use the approximation of determining the intersection of a vertical transition with the final state potential energy surface to estimate the largest Franck-Condon factor. This short-cut is good for transitions to highly excited vibrational

states, but is poor for low lying vibrational states. Of course it is always best to calculate the Franck-Condon integrals directly, using the vibrational wave functions (if the potential energy surfaces are known)

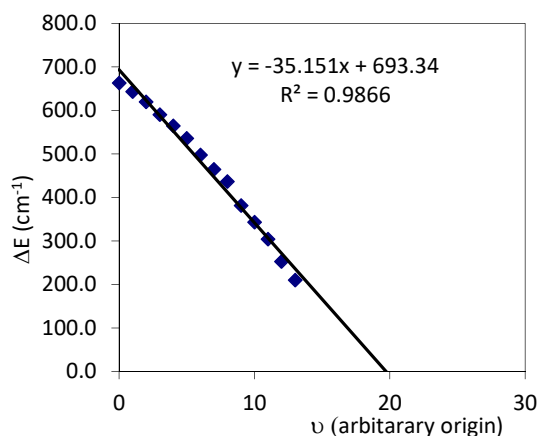
15. The Schumann-Runge band for molecular oxygen is in the UV-region of the spectrum. The wave numbers for the  ${}^3\Sigma_u^- \leftarrow {}^3\Sigma_g^-$  transitions are given in the table below. The corresponding vibrational quantum numbers are not known. The ground state dissociates into two ground state  ${}^3P$  oxygen atoms, and the  ${}^3\Sigma_u^-$  excited state dissociates into a  ${}^3P$  and a  ${}^1D$  oxygen atom. Calculate (a) the dissociation energy of the ground state (the bond strength). (b). Estimate the dissociation energy of the excited state by assuming the first observed transition is for  $v \cong 0$ . The atomic excitation energy,  ${}^3P \rightarrow {}^1D$  is 1.9674 eV, 15867.9  $\text{cm}^{-1}$ , or 189.82 kJ/mol.

$\tilde{\nu}$ ( $\text{cm}^{-1}$ )	50062.6	50725.4	51369.0	51988.6	52579.0	53143.4	53679.6	54177.0
continued	54641.8	55078.2	55460.0	55803.1	56107.3	56360.3	56570.6	

*Answer:* The plan is to use a Birge-Sponer extrapolation following Example 28.2.2 and then Eq. 28.2.6 to determine the dissociation energies.

The adjacent differences are calculated in the following spreadsheet with the corresponding Birge-Sponer extrapolation. An arbitrary quantum number of zero is assigned to the first transition, since the vibrational quantum numbers are not known.

$v$	$\tilde{\nu}_v$ ( $\text{cm}^{-1}$ )	$\Delta\tilde{\nu}_v$ ( $\text{cm}^{-1}$ )
0	50062.6	662.8
1	50725.4	643.6
2	51369.0	619.6
3	51988.6	590.4
4	52579.0	564.4
5	53143.4	536.2
6	53679.6	497.4
7	54177.0	464.8
8	54641.8	436.4
9	55078.2	381.8
10	55460.0	343.1
11	55803.1	304.2
12	56107.3	253.0
13	56360.3	210.3
	56570.6	



slope	-35.15121	693.34	b
±	1.1829486	9.0478167	±
r <sup>2</sup>	0.9865918	17.842535	s(y)
F	882.97582	12	df
SS <sub>reg</sub>	281100.7	3820.2727	SS <sub>residual</sub>

(a). Using Eq. 28.2.17, the slope gives the anharmonicity:  $\chi_e^{\text{ex}} \tilde{\nu}_e^{\text{ex}} = -\frac{1}{2} \text{slope} = 17.58 \pm 0.59 \text{ cm}^{-1}$

Using Eq. 28.2.18:  $v_{\text{cl}} = \frac{\Delta\tilde{\nu}_0}{2\chi_e^{\text{ex}} \tilde{\nu}_e^{\text{ex}}} = \frac{693.34}{35.1512} = 19.73 \pm 0.71$

Using Eq. 28.2.19:  $\text{area} = \frac{1}{2} \Delta\tilde{\nu}_0 v_{\text{cl}} = \frac{1}{2} (693.34)(19.73) = 6839.8 \pm 262 \text{ cm}^{-1}$

Using Eq. 28.2.20, the transition wave number at the convergence limit is:

$$\begin{aligned}\tilde{\nu}_{\infty 0} &= \tilde{\nu}_{00} + \text{area} = 50062.6 \text{ cm}^{-1} + 6839.8 \text{ cm}^{-1} \\ &= 56902.4 \pm 262 \text{ cm}^{-1} = 7.055 \pm 0.032 \text{ eV}\end{aligned}$$

Using Eq. 28.2.6, the bond energy of the ground state is:

$$\begin{aligned}\text{in cm}^{-1}: \quad \tilde{D}_0 &= \tilde{\nu}_{\infty 0} - \Delta\tilde{E}_{\text{atomic}} = (56902.4 \pm 262 \text{ cm}^{-1}) - 15867.9 \text{ cm}^{-1} = 41035 \pm 262 \text{ cm}^{-1} \\ \text{in eV}: \quad D_0 &= \Delta E(j, \infty \leftarrow i, 0) - \Delta E_{\text{atomic}} = (7.055 \pm 0.032 \text{ eV}) - 1.9674 \text{ eV} = 5.0876 \pm 0.032 \text{ eV} \\ \text{in kJ mol}^{-1}: &= 490.9 \pm 3.1 \text{ kJ mol}^{-1}\end{aligned}$$

Notice that the Birge-Sponer plot has significant systematic curvature, and the convergence limit by visual extrapolation appears to be less than  $\nu = 19$ , which decreases the calculated ground and excited state dissociation energies. The literature ground state dissociation energy is 5.126 eV.

(b). If  $\nu \cong 0$  for the first transition, then the excited state dissociation energy is the area under the Birge-Sponer curve, Eq. 28.2.19:

$$\tilde{D}_0^{\text{ex}} \cong \text{area} = 6840 \text{ cm}^{-1} = 0.85 \text{ eV}$$

which suffices as a lower limit of the true excited state dissociation energy. The error is within a few multiples of  $\tilde{\nu}_0^{\text{ex}}$ , which is 0.082 eV. If  $\tilde{\nu}_0^{\text{ex}}$  is  $662.8 \text{ cm}^{-1}$  as we have assumed, then using Eq. 27.5.11,  $\tilde{\nu}_e^{\text{ex}} \cong \tilde{\nu}_0^{\text{ex}} + 2\chi_e^{\text{ex}} \tilde{\nu}_0^{\text{ex}} = 662.8 \text{ cm}^{-1} + 35.15 \text{ cm}^{-1} = 698.0 \text{ cm}^{-1}$ . The literature value of  $\tilde{\nu}_e^{\text{ex}}$  is  $799.1 \text{ cm}^{-1}$ , which suggests that the first observed transition is actually for  $\nu = 3$ .

16. For SiS the wave numbers for the  $E^1\Sigma^+ \leftarrow X^1\Sigma^+$  transitions are given in the table below.<sup>6</sup> The ground state is labeled as the X-state and this excited state, which has the same symmetry, is the E-state. Assume that the corresponding vibrational quantum numbers are not known. The ground and excited states dissociate into two ground-state  $^3\text{P}$  atoms. Calculate the dissociation energy of the ground state (the bond strength).

---

$\tilde{\nu} \text{ (cm}^{-1}\text{)}$	44482.8	44857.6	45227.0	45592.2	45952.8	46308.3	46657.7	47001.0	47337.9	47664.0
--	---------	---------	---------	---------	---------	---------	---------	---------	---------	---------

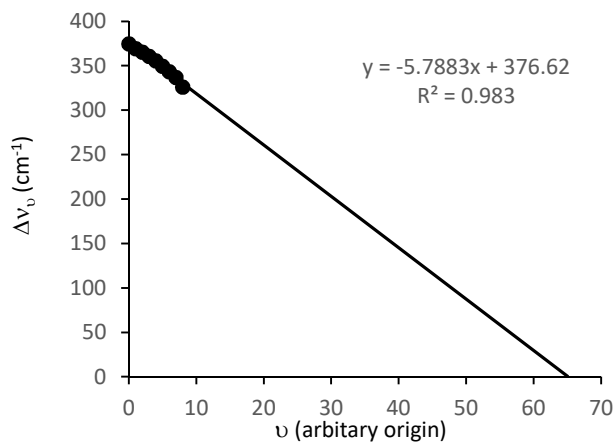
---

*Answer:* The plan is to use a Birge-Sponer extrapolation following Example 28.2.2 and then Eq. 28.2.6 to determine the dissociation energies. The first transition is assigned an arbitrary vibrational quantum number of zero for the purposes of the extrapolation.

The adjacent differences are calculated in the following spreadsheet with the corresponding Birge-Sponer extrapolation. An arbitrary quantum number of zero is assigned to the first transition, since the vibrational quantum numbers are not known. Because we are assigning an arbitrary vibrational quantum number, the intercept is not the fundamental vibration frequency. The extrapolation to the convergence limit works out just fine, however.

$\nu$	$\nu_\nu$ (cm <sup>-1</sup> )	$\Delta\nu_\nu$ (cm <sup>-1</sup> )
0	44482.8	374.8
1	44857.6	369.4
2	45227	365.2
3	45592.2	360.6
4	45952.8	355.5
5	46308.3	349.4
6	46657.7	343.3
7	47001	336.9
8	47337.9	326.1
9	47664	

slope	-5.7883	376.62	b
$\pm$	0.2873	1.3679	$\pm$
$r^2$	0.9830	2.2256	$s(y)$
F	405.8631	7	df
$SS_{reg}$	2010.2882	34.6718	$SS_{residual}$



(a). Using Eq. 28.2.17, the slope gives the anharmonicity:  $\chi_e^{\text{ex}} \tilde{\nu}_e^{\text{ex}} = -\frac{1}{2} \text{slope} = 2.894 \pm 0.14 \text{ cm}^{-1}$

$$\text{Using Eq. 28.2.18: } \nu_{cl} = \frac{\tilde{\Delta\nu}_0}{2\chi_e^{\text{ex}} \tilde{\nu}_e^{\text{ex}}} = \frac{376.62}{5.7883} = 65.07 \pm 3.24$$

Using Eq. 28.2.19:  $\text{area} = \frac{1}{2} \tilde{\Delta\nu}_0 \nu_{cl} = \frac{1}{2} (376.62)(65.07) = 12250 \pm 612 \text{ cm}^{-1}$

Using Eq. 28.2.20, the transition wave number at the convergence limit is:

$$\begin{aligned} \tilde{\nu}_{\infty 0} &= \tilde{\nu}_{00} + \text{area} = 44482.8 \text{ cm}^{-1} + 12250 \text{ cm}^{-1} \\ &= 56732.8 \pm 612 \text{ cm}^{-1} = 7.034 \pm 0.076 \text{ eV} \end{aligned}$$

Since the excited state gives ground state atoms,  $\Delta\tilde{E}_{\text{atomic}}$  is zero for this transition. Using Eq. 28.2.6, the bond energy of the ground state is:

$$\begin{aligned} \text{in cm}^{-1}: \quad \tilde{D}_0 &= \tilde{\nu}_{\infty 0} - \Delta\tilde{E}_{\text{atomic}} = 56732.8 \pm 612 \text{ cm}^{-1} \\ \text{in eV}: \quad D_0 &= \Delta E(j, \infty \leftarrow i, 0) - \Delta E_{\text{atomic}} = 7.034 \pm 0.076 \text{ eV} \\ \text{in kJ mol}^{-1}: &= 678.7 \pm 7.3 \text{ kJ mol}^{-1} \end{aligned}$$

Notice that the convergence limit is a long extrapolation on the Birge-Spinner plot, giving large uncertainties. The last data point also shows some downward curvature, which would decrease the convergence limit and corresponding dissociation energies. The literature ground state dissociation energy, which is based on the same data is 6.72 eV, which takes into account some of the observed curvature through a second anharmonicity correction.

**17.** Vibrational potential functions commonly deviate from Morse behavior. One possibility is the appearance of a maximum, Figure P28.17.1a. One cause of a maximum is a strong Van der Waals repulsion at large distances, but strong bonding interactions at short distances.<sup>5</sup> Referring to Figure 26.2.4, strong electron-electron repulsion increases the potential energy at large  $R$ , possibly giving a maximum. A second cause, especially for excited states, is an avoided crossing between a bound-state potential energy curve and a repulsive state, Figure P28.17.1b. An example is a state of an alkali halide that tends to dissociate to ions, but because of the curve crossing dissociates to atoms instead.<sup>5</sup> Discuss the effect of a potential maximum on the spectroscopic determination of the dissociation energy of the bound state.

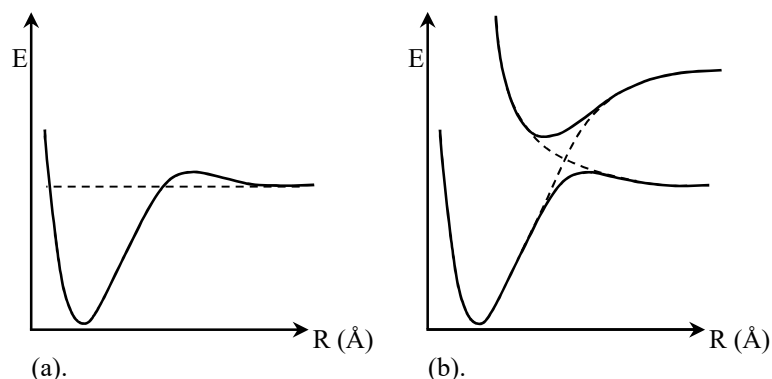
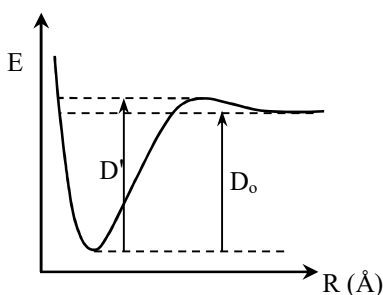


Figure P28.17.1: (a). Some vibrational potential energy curves have a maximum. (b). One cause is an avoided crossing.

*Answer:* The plan is to consider what the results of a Birge-Sponer extrapolation would yield for the dissociation energy.

Birge Sponer extrapolation yields the dissociation energy  $D'$ , which is greater than the true dissociation energy  $D_0$ . The relationship is diagrammed below. Such circumstances are not uncommon, especially upon comparisons of spectroscopic and thermodynamically obtained values.<sup>1</sup>



18. The electronic absorption spectrum of water has a Rydberg series that start with the configuration  $\dots(3a_1)^2(1b_1)^1(3p)^1$  for a 3p-orbital on the O-atom. See Figure 26.6.4 for the molecular orbital diagram. Is the Rydberg series consistent with the ultraviolet photoelectron spectrum, UPS, of water shown in Figure 28.5.4b? The series has transitions:

$$\tilde{\nu}_n = 101786 \text{ cm}^{-1} - \frac{\mathfrak{R}_H}{(n - 0.7)^2} \quad n = 3, 4, 5, \dots$$

*Answer:* The plan is to note that the Rydberg ionization limit corresponds to the formation of the molecular ion.

The ionization limit converted to eV is:  $\tilde{\nu}_n = 101786 \text{ cm}^{-1}(1 \text{ eV}/8065.5 \text{ cm}^{-1}) = 12.62 \text{ eV}$  which agrees exactly with the first ionization potential from the UPS spectrum in Figure 28.5.4b. Rydberg series don't necessarily give the ground state of the molecular ion, but such is the case in this example.

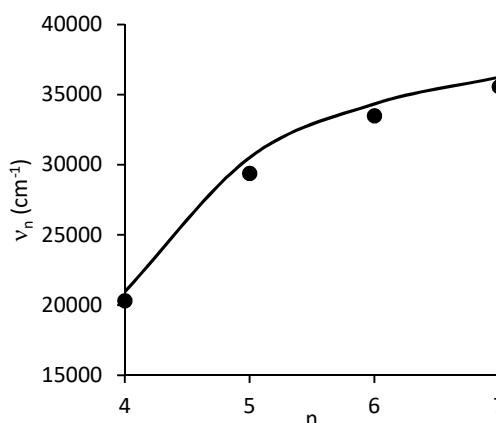
19. The diatomic molecule  $\text{Na}_2$  has a Rydberg series in the electronic absorption spectrum. The ionization limit gives the ground state of the molecular ion,  $\text{Na}_2^+$ . The ionization limit from the Rydberg series and the ionization potential measured using UPS should be identical for the specific excited state of the molecular ion. The quantum numbers of the Rydberg transitions and the wave numbers are given in the table below. Determine the ionization potential to form  $\text{Na}_2^+$ . Compare the value to the ionization potential determined using UPS, which is 4.90 eV (see Problem 37 for the reference to the literature value).

n	4	5	6	7
$\tilde{\nu}_n$	20320.02	29382	33486.8	35557

*Answer:* The plan is to fit the data to the Rydberg series expression, Eq. 28.2.22. We first write a spreadsheet to approximate the fit coefficients and then use non-linear least squares curve fitting.

A spreadsheet to do an approximate curve fit is shown below. As usual the goal is to minimize the sum of squared residuals, which is calculated in cell E11. The fit parameters, which are the wave number of the ionization limit  $\tilde{\nu}_1$  in cell C3 and the quantum defect  $c$  in cell C4, are varied to achieve an approximate fit. With patience, or using Goal Seek, this guessing procedure is sufficient to complete the fit, but we only need to derive approximate fit values at this point.

A1	B	C	D	E	F
2	$\tilde{\nu}_H$	109737.32			
3	$\nu_1$	40000	$\text{cm}^{-1}$	4.959	eV
4	$c$	-1.6			
5	n	$\nu_n$ ( $\text{cm}^{-1}$ )	fit	$r^2$	
6	4	20320.02	20948.4	394839.7	
7	5	29382	30507.2	1265968.5	
8	6	33486.8	34331.8	713940.9	
9	7	35557	36236.7	462016.0	
10					
11			sum $r^2$	2836765.1	



Using approximate values close to those from the spreadsheet, a curve fit using the “Nonlinear Least Squares Curve Fitting” applet on the textbook Web site or companion CD is done using the functional form “ $a+c/(x+b)^2$ ” as set up below with a constant  $c$  value for the Rydberg constant.

Input data pairs:

4	20320.02
5	29382
6	33486.8
7	35557

Fit function:  $a+c/(x+b)^2$

Parameter guesses:

a = 20000

b = -1

c = -109737.3  Fixed

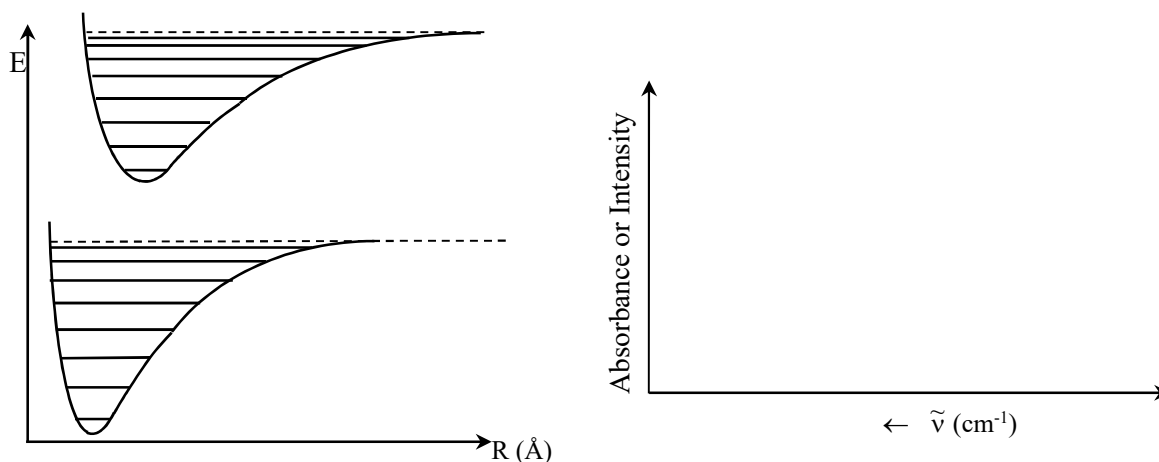
```

===== Results =====
a= 39107 +- 194
b= -1.5887 +- 0.023
-----
Output Data
-----
x      y      y(fit)  residual
4.0    20320.02  20233.351  86.6684
5.0    29382.0   29676.904 -294.904
6.0    33486.8   33467.758  19.0413
7.0    35557.0   35359.440  197.559
-----
sum of squared residuals= 133900
stand. dev. y values= 258.7
correlation between a & b= -0.7453

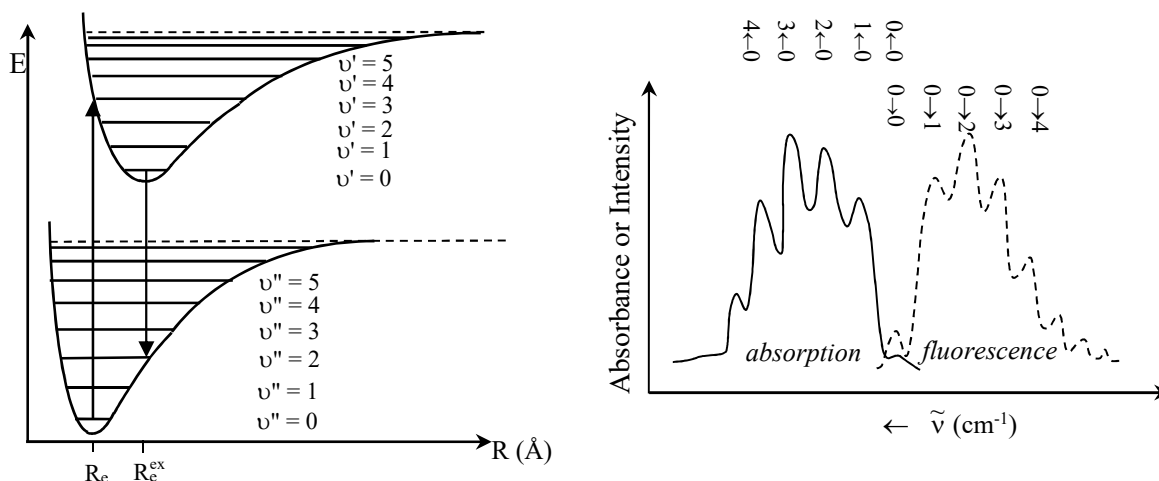
```

Notice that the guesses don't need to be very close to the final values; we just used the spreadsheet to get a reasonable estimate for  $c$  (small negative). The curve fit results give the ionization limit,  $\tilde{\nu}_1 = 39107 \pm 194 \text{ cm}^{-1} = 4.849 \pm 0.024 \text{ eV}$ , which is in excellent agreement with the UPS derived ionization potential.

20. Using the potential energy curves shown below, predict the most intense vibrational fine-structure transitions in the absorption and fluorescence spectra. Draw the corresponding absorption and fluorescence spectra. Show four of the intense transitions in each of the spectra. Label each transition in the energy level diagram with the vibrational quantum numbers for the transition and each corresponding peak in the spectrum (e.g.  $4 \leftarrow 0$ ).



*Answer:* The plan is to draw in the vertical transitions to predict the vibrational fine-structure transition with the largest Franck-Condon factors.



The most probable internuclear separation in the  $v'' = 0$  vibrational state of the electronic ground state is the middle of the potential energy well, giving the starting point for the vertical transition in absorption as  $R_e$ . The most intense transition in absorption is to  $v' = 3$ , as shown in

the figure above. Transitions to other adjacent vibrational levels typically have comparable intensities. The vertical transition just predicts the most intense. The most probable internuclear separation in the  $\nu' = 0$  vibrational state of the first excited electronic state is also in the middle of the potential energy well, giving the starting point for the vertical transition in absorption as  $R_e^{\text{ex}}$ . The most intense transition in fluorescence is to  $\nu'' = 2$ , as shown in the figure above.

21. We took a short cut in the derivation of Eq. 28.2.13 by working in analogy with Eq. 27.5.12. In this problem we derive Eq. 28.2.13 directly from the term values of the adjacent transitions. The energy of the  $\nu'' = 0$  level of the ground electronic state is  $\tilde{E}_0$ . The energy difference from the minimum energy of the ground state potential energy curve to the minimum energy of the excited state potential energy curve, that is the energy without vibration, is  $\tilde{T}_e^{\text{ex}}$ . The energy of the  $\nu'$  vibrational level of the excited state is  $\tilde{E}_{\nu'}^{\text{ex}}$ , neglecting rotation:

$$\tilde{E}_{\nu'}^{\text{ex}} = \tilde{T}_e^{\text{ex}} + \tilde{\nu}_e^{\text{ex}} (\nu' + \frac{1}{2}) - \chi_e^{\text{ex}} \tilde{\nu}_e^{\text{ex}} (\nu' + \frac{1}{2})^2 \quad \text{P28.14.1}$$

The energy of an electronic transition from the  $\nu'' = 0$  level of the ground electronic state to the  $\nu'$  vibrational level of the excited state is:

$$\Delta\tilde{E}(j, \nu' \leftarrow i, 0) = \tilde{E}_{\nu'}^{\text{ex}} - \tilde{E}_0 = \tilde{T}_e^{\text{ex}} + \tilde{\nu}_e^{\text{ex}} (\nu' + \frac{1}{2}) - \chi_e^{\text{ex}} \tilde{\nu}_e^{\text{ex}} (\nu' + \frac{1}{2})^2 - \tilde{E}_0 \quad \text{P28.14.2}$$

where the fundamental vibration frequency  $\tilde{\nu}_e^{\text{ex}}$  and anharmonicity  $\chi_e^{\text{ex}} \tilde{\nu}_e^{\text{ex}}$  are for the excited state. Consider two adjacent transitions:  $j, \nu + 1 \leftarrow i, 0$  and  $j, \nu \leftarrow i, 0$ . The adjacent energy difference is:

$$\Delta\tilde{\nu}_\nu = \Delta\tilde{E}(j, \nu + 1 \leftarrow i, 0) - \Delta\tilde{E}(j, \nu \leftarrow i, 0) \quad \text{P28.14.3}$$

$$(a). \text{ Prove that: } \Delta\tilde{\nu}_\nu = \tilde{\nu}_e^{\text{ex}} - \chi_e^{\text{ex}} \tilde{\nu}_e^{\text{ex}} [(\nu + \frac{1}{2}) + 1]^2 + \chi_e^{\text{ex}} \tilde{\nu}_e^{\text{ex}} (\nu + \frac{1}{2})^2 \quad \text{P28.14.4}$$

(b). Using  $((\nu + \frac{1}{2}) + 1)^2 = (\nu + \frac{1}{2})^2 + 2(\nu + \frac{1}{2}) + 1$ , starting with Eq. P28.14.4 prove that:

$$\Delta\tilde{\nu}_\nu = (h\tilde{\nu}_e^{\text{ex}} - 2\chi_e^{\text{ex}} \tilde{\nu}_e^{\text{ex}}) - 2\chi_e^{\text{ex}} \tilde{\nu}_e^{\text{ex}} \nu \quad (28.2.13)$$

(c). Label  $\tilde{E}_0$ ,  $\tilde{E}_{\nu'}^{\text{ex}}$ ,  $\tilde{T}_e^{\text{ex}}$ ,  $\Delta\tilde{E}(j, \nu + 1 \leftarrow i, 0)$ ,  $\Delta\tilde{E}(j, \nu \leftarrow i, 0)$ , and  $\Delta\tilde{\nu}_\nu$  on a plot of the ground and excited state potential energy curves. Pick a convenient arbitrary  $\nu$  for your plot.

*Answer:* (a). The adjacent energy difference is:

$$\Delta\tilde{\nu}_\nu = \Delta\tilde{E}(j, \nu + 1 \leftarrow i, 0) - \Delta\tilde{E}(j, \nu \leftarrow i, 0) = [\tilde{E}_{\nu+1}^{\text{ex}} - \tilde{E}_0] - [\tilde{E}_\nu^{\text{ex}} - \tilde{E}_0] = \tilde{E}_{\nu+1}^{\text{ex}} - \tilde{E}_\nu^{\text{ex}} \quad \text{P28.14.5}$$

Substitution of Eq. P28.14.1 evaluated at  $\nu + 1$  and  $\nu$  into Eq. P28.14.5 and cancelling the common  $\tilde{T}_e^{\text{ex}}$  terms gives the adjacent energy difference as:

$$\Delta\tilde{\nu}_\nu = \tilde{\nu}_e^{\text{ex}} (\nu + 1 + \frac{1}{2}) - \chi_e^{\text{ex}} \tilde{\nu}_e^{\text{ex}} (\nu + 1 + \frac{1}{2})^2 - \tilde{\nu}_e^{\text{ex}} (\nu + \frac{1}{2}) + \chi_e^{\text{ex}} \tilde{\nu}_e^{\text{ex}} (\nu + \frac{1}{2})^2$$

Cancelling common terms and rearranging  $(\nu + 1 + \frac{1}{2})$  to give  $((\nu + \frac{1}{2}) + 1)$  gives Eq. P28.14.4:

$$\Delta\tilde{\nu}_\nu = \tilde{\nu}_e^{\text{ex}} - \chi_e^{\text{ex}} \tilde{\nu}_e^{\text{ex}} [(\nu + \frac{1}{2}) + 1]^2 + \chi_e^{\text{ex}} \tilde{\nu}_e^{\text{ex}} (\nu + \frac{1}{2})^2 \quad (\text{P28.14.4})$$

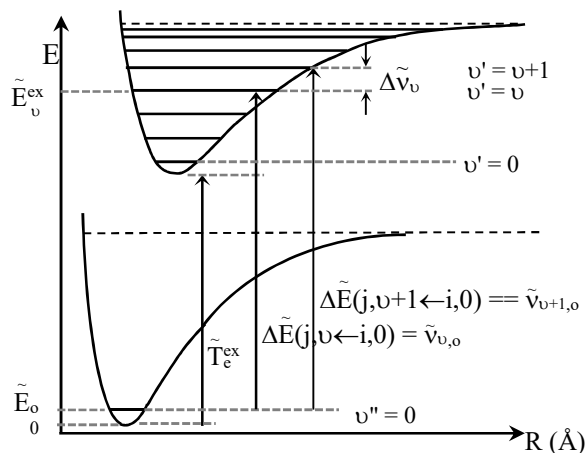
(b). As in Eq. 27.5.9, using  $((\nu + \frac{1}{2}) + 1)^2 = (\nu + \frac{1}{2})^2 + 2(\nu + \frac{1}{2}) + 1$  and cancelling the resulting common terms gives:

$$\Delta\tilde{\nu}_\nu = \tilde{\nu}_e^{\text{ex}} - \chi_e^{\text{ex}} \tilde{\nu}_e^{\text{ex}} [(\nu + \frac{1}{2})^2 + 2(\nu + \frac{1}{2}) + 1] + \chi_e^{\text{ex}} \tilde{\nu}_e^{\text{ex}} (\nu + \frac{1}{2})^2 = \tilde{\nu}_e^{\text{ex}} - \chi_e^{\text{ex}} \tilde{\nu}_e^{\text{ex}} (2\nu + 2)$$

Rearranging the last equation into the form of a straight line gives Eq. 28.2.13:

$$\Delta\tilde{\nu}_\nu = (\hbar\tilde{\nu}_e^{\text{ex}} - 2\chi_e^{\text{ex}}\tilde{\nu}_e^{\text{ex}}) - 2\chi_e^{\text{ex}}\tilde{\nu}_e^{\text{ex}}\nu \quad (28.2.13)$$

(c).



22. The next three problems discuss errors in the Birge-Sponer extrapolation procedure and why different authors chose different variables to plot along the horizontal axis,  $\nu$ ,  $\nu + \frac{1}{2}$ , or  $\nu + 1$ . The vibrational fine-structure in an electronic absorption spectrum converges to a limit that is the sum of the dissociation energy of the ground state of the molecule and the atomic excitation energy. The convergence limit is equivalent to the sum of  $\tilde{\nu}_{00}$  and the excited state dissociation energy, Eq. 28.2.8. Reference to Figure 28.2.5 shows that the excited state dissociation energy is the sum of all the adjacent wave number differences up to the convergence limit:

$$\Delta\tilde{E}(j, \infty \leftarrow i, 0) = \tilde{D}_0 + \Delta\tilde{E}_{\text{atomic}} = \tilde{\nu}_{00} + \tilde{D}_0^{\text{ex}} = \tilde{\nu}_{00} + \sum_{\nu=0}^{\infty} \Delta\tilde{\nu}_\nu \quad \text{P28.22.1}$$

Based on the sum of adjacent differences, the Birge-Sponer extrapolation may be viewed from a different perspective. A graphical interpretation of Figure 28.1.20 allows a convenient calculation of the sum in Eq. P28.22.1. Consider a rectangle of unit width drawn at each data point, Figure P28.22.1.

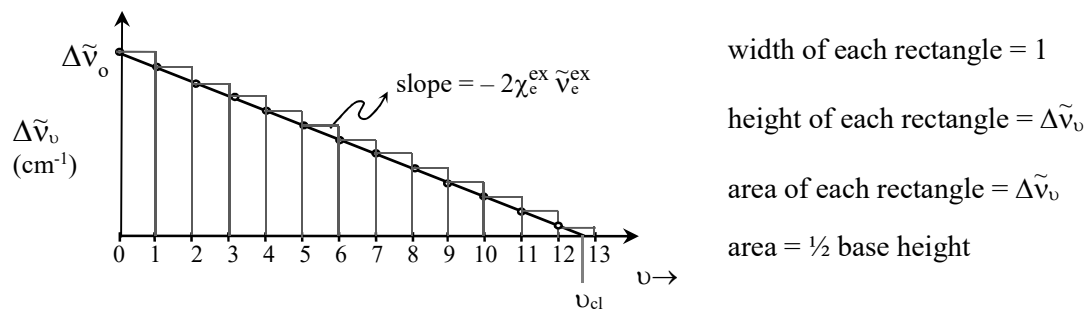


Figure P28.22.1: The excited state dissociation energy  $\tilde{D}_0^{\text{ex}}$  is given by the sum of adjacent energy differences, which is conveniently calculated as the triangular area under the plot of  $\Delta\tilde{\nu}_\nu$  versus  $\nu$ .

The area of each rectangle is the height multiplied by the width. The sum of all the successive differences is then equal to the total area of all the rectangles. The total area is approximated as the triangle with the area given by  $\frac{1}{2}$  base  $\cdot$  height:

$$\sum_{\nu=0}^{\infty} \Delta \tilde{\nu}_{\nu} = \text{area} = \frac{1}{2} \Delta \tilde{\nu}_0 \nu_{cl} \quad (28.2.19)$$

Compare this approximate result, which we also gave as Eq. 28.2.19, to the exact result using Eq. 28.2.15. Express your answer in terms of the anharmonicity,  $\chi_e^{\text{ex}} \tilde{\nu}_e^{\text{ex}}$ .

*Answer:* The plan is to compare  $\Delta \tilde{\nu}_0$  to  $\tilde{\nu}_e^{\text{ex}}$  using Eq. 28.2.16.

The exact result is given by Eq. 28.2.15:  $\tilde{D}_0^{\text{ex}} = \frac{1}{2} \tilde{\nu}_e^{\text{ex}} \nu_{cl}$ . Substituting Eq. 28.2.16:

$$\Delta \tilde{\nu}_0 = \tilde{\nu}_e^{\text{ex}} - 2\chi_e^{\text{ex}} \tilde{\nu}_e^{\text{ex}}$$

into Eq. 28.2.16 gives:

$$\tilde{D}_0^{\text{ex}} = \frac{1}{2} \tilde{\nu}_e^{\text{ex}} \nu_{cl} = \frac{1}{2} (\Delta \tilde{\nu}_0 + 2\chi_e^{\text{ex}} \tilde{\nu}_e^{\text{ex}}) \nu_{cl} = \frac{1}{2} \Delta \tilde{\nu}_0 \nu_{cl} + \chi_e^{\text{ex}} \tilde{\nu}_e^{\text{ex}} \nu_{cl}$$

The error in using Eq. 28.2.19 is then  $\chi_e^{\text{ex}} \tilde{\nu}_e^{\text{ex}} \nu_{cl}$ , which is typically small since the anharmonicity is usually a small fraction of the fundamental vibration frequency.

**23.** Birge-Sponer extrapolations are plotted as a function of the vibrational quantum number  $\nu$  based on the following the linear forms:

$$\Delta \tilde{\nu}_{\nu} = (\tilde{\nu}_e^{\text{ex}} - 2\chi_e^{\text{ex}} \tilde{\nu}_e^{\text{ex}}) - 2\chi_e^{\text{ex}} \tilde{\nu}_e^{\text{ex}} \nu \quad (28.2.13)$$

$$\text{or equivalently} \quad \Delta \tilde{\nu}_{\nu} = \Delta \tilde{\nu}_0 - 2\chi_e^{\text{ex}} \tilde{\nu}_e^{\text{ex}} \nu \quad (28.2.17)$$

In the previous problem we discuss a graphical interpretation that leads to the use of the triangular area under the Birge-Sponer curve to estimate the dissociation energy of the excited state. This graphical interpretation in Figure P28.22.1 shows a problem in associating the area of each rectangle with the overall area; each rectangle has a small portion above the curve-fit line. Some authors suggest doing the curve fit versus  $\nu + \frac{1}{2}$  to limit the error in this area calculation, Figure P28.23.1.

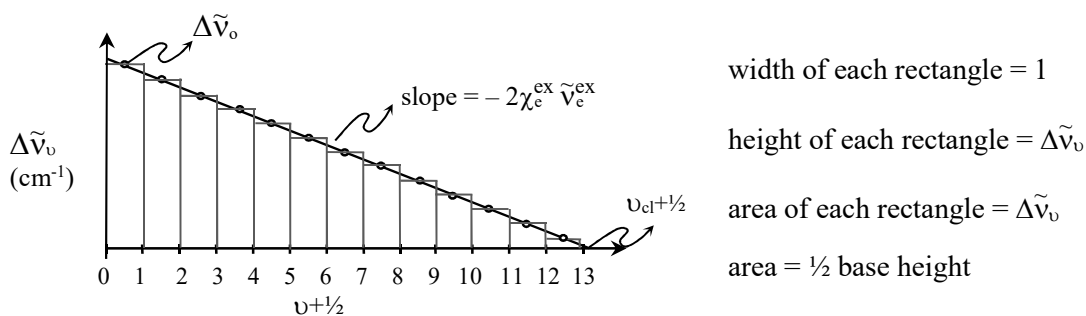


Figure P28.23.1: The excited state dissociation energy  $\tilde{D}_0^{\text{ex}}$  is given by the sum of adjacent energy differences, which is conveniently calculated as the triangular area under the plot of  $\Delta \tilde{\nu}_{\nu}$  versus  $\nu + \frac{1}{2}$ .

The dissociation energy of the excited state is given approximately by area  $\tilde{D}_0^{\text{ex}} = \frac{1}{2} \Delta\tilde{\nu}_0 \nu_{\text{cl}}$ , where  $\Delta\tilde{\nu}_0$  is taken as the first data point and  $\nu_{\text{cl}} = (\text{x-intercept}) - \frac{1}{2}$ . This result is identical to the result taken from the plot versus  $\nu$  discussed in the Example 28.2.2. However, some authors instead use:

$$\tilde{D}_0^{\text{ex}} \cong \text{area} = \frac{1}{2}(\text{y-intercept})(\text{x-intercept})$$

Evaluate the error in the corresponding calculation of  $\tilde{D}_0^{\text{ex}}$  by showing that:

$$\tilde{D}_0^{\text{ex}} = \frac{1}{2} (\text{y-intercept})(\text{x-intercept}) - \frac{1}{4} \tilde{\nu}_e^{\text{ex}} + \frac{1}{2} \chi_e^{\text{ex}} \tilde{\nu}_e^{\text{ex}} \nu_{\text{cl}} + \frac{1}{4} \chi_e^{\text{ex}} \tilde{\nu}_e^{\text{ex}}$$

*Answer:* The plan is to compare the y-intercept to  $\tilde{\nu}_e^{\text{ex}}$  using Eq. 28.2.13. Make the substitution  $x = \nu + \frac{1}{2}$ , where x is the variable plotted along the horizontal axis.

$$\text{The basis of the Birge-Sponer plot is Eq. 28.2.13: } \Delta\tilde{\nu}_\nu = (\tilde{\nu}_e^{\text{ex}} - 2\chi_e^{\text{ex}} \tilde{\nu}_e^{\text{ex}}) - 2\chi_e^{\text{ex}} \tilde{\nu}_e^{\text{ex}} \nu$$

To switch variables, rearrange to give  $\nu = x - \frac{1}{2}$  and substitute into the previous equation:

$$\Delta\tilde{\nu}_\nu = (\tilde{\nu}_e^{\text{ex}} - 2\chi_e^{\text{ex}} \tilde{\nu}_e^{\text{ex}}) - 2\chi_e^{\text{ex}} \tilde{\nu}_e^{\text{ex}} (x - \frac{1}{2}) = (\tilde{\nu}_e^{\text{ex}} - \chi_e^{\text{ex}} \tilde{\nu}_e^{\text{ex}}) - 2\chi_e^{\text{ex}} \tilde{\nu}_e^{\text{ex}} x$$

with the y-intercept =  $(\tilde{\nu}_e^{\text{ex}} - \chi_e^{\text{ex}} \tilde{\nu}_e^{\text{ex}})$  and the x-intercept =  $\nu_{\text{cl}} + \frac{1}{2}$ .

The exact result for the dissociation energy of the excited state is given by Eq. 28.2.15:

$\tilde{D}_0^{\text{ex}} = \frac{1}{2} \tilde{\nu}_e^{\text{ex}} \nu_{\text{cl}}$ . Solving the y- and x-intercepts for  $\tilde{\nu}_e^{\text{ex}}$  and  $\nu_{\text{cl}}$  gives:

$$\begin{aligned} \tilde{D}_0^{\text{ex}} &= \frac{1}{2} \tilde{\nu}_e^{\text{ex}} \nu_{\text{cl}} = \frac{1}{2} (\text{y-intercept} + \chi_e^{\text{ex}} \tilde{\nu}_e^{\text{ex}})(\text{x-intercept} - \frac{1}{2}) \\ &= \frac{1}{2} (\text{y-intercept})(\text{x-intercept}) - \frac{1}{4} (\text{y-intercept}) + \frac{1}{2} \chi_e^{\text{ex}} \tilde{\nu}_e^{\text{ex}}(\text{x-intercept}) - \frac{1}{4} \chi_e^{\text{ex}} \tilde{\nu}_e^{\text{ex}} \\ &= \frac{1}{2} (\text{y-intercept})(\text{x-intercept}) - \frac{1}{4} (\tilde{\nu}_e^{\text{ex}} - \chi_e^{\text{ex}} \tilde{\nu}_e^{\text{ex}}) + \frac{1}{2} \chi_e^{\text{ex}} \tilde{\nu}_e^{\text{ex}}(\nu_{\text{cl}} + \frac{1}{2}) - \frac{1}{4} \chi_e^{\text{ex}} \tilde{\nu}_e^{\text{ex}} \\ &= \frac{1}{2} (\text{y-intercept})(\text{x-intercept}) - \frac{1}{4} \tilde{\nu}_e^{\text{ex}} + \frac{1}{2} \chi_e^{\text{ex}} \tilde{\nu}_e^{\text{ex}} \nu_{\text{cl}} + \frac{1}{4} \chi_e^{\text{ex}} \tilde{\nu}_e^{\text{ex}} \end{aligned}$$

The last term is negligible. The error in the term  $\frac{1}{2} \chi_e^{\text{ex}} \tilde{\nu}_e^{\text{ex}} \nu_{\text{cl}}$  is typically small since the anharmonicity is usually a small fraction of the fundamental vibration frequency. The error in using the y- and x-intercepts directly is dominated by the term  $-\frac{1}{4} \tilde{\nu}_e^{\text{ex}}$ . Assuming  $\tilde{\nu}_e^{\text{ex}}$  is typically on the order of  $\sim 2000 \text{ cm}^{-1}$ :

$$\text{error} = -\frac{1}{4} \tilde{\nu}_e^{\text{ex}} = -\frac{1}{4} (2000 \text{ cm}^{-1})(1 \text{ eV}/8065.5 \text{ cm}^{-1}) = -0.06 \text{ eV}$$

which is often smaller than other sources of error. In summary, using  $\tilde{D}_0^{\text{ex}} = \frac{1}{2} \tilde{\nu}_e^{\text{ex}} \nu_{\text{cl}}$  is best, but using  $\frac{1}{2} \Delta\tilde{\nu}_0 \nu_{\text{cl}}$  introduces small amounts of error. Using  $\frac{1}{2} (\text{y-intercept})(\text{x-intercept})$  from the plot versus  $\nu + \frac{1}{2}$  introduces small but significant error.

**24.** As an alternate to the Birge-Sponer plot where  $\Delta\tilde{\nu}_\nu$  is plotted versus  $\nu$ , show that a plot of  $\Delta\tilde{\nu}_\nu$  versus  $\nu + 1$  gives  $\tilde{\nu}_e^{\text{ex}}$  directly from the intercept.

*Answer:* The plan is to compare the y-intercept to  $\tilde{\nu}_e^{\text{ex}}$  using Eq. 28.2.13. Make the substitution  $x = \nu + 1$ , where x is the variable plotted along the horizontal axis.

The basis of the Birge-Sponer plot is Eq. 28.2.13:  $\Delta\tilde{\nu}_v = (\tilde{\nu}_e^{\text{ex}} - 2\chi_e^{\text{ex}} \tilde{\nu}_e^{\text{ex}}) - 2\chi_e^{\text{ex}} \tilde{\nu}_e^{\text{ex}} v$

To switch variables, rearrange to give  $v = x - 1$  and substitute into the previous equation:

$$\Delta\tilde{\nu}_v = (\tilde{\nu}_e^{\text{ex}} - 2\chi_e^{\text{ex}} \tilde{\nu}_e^{\text{ex}}) - 2\chi_e^{\text{ex}} \tilde{\nu}_e^{\text{ex}} (x - 1) = \tilde{\nu}_e^{\text{ex}} - 2\chi_e^{\text{ex}} \tilde{\nu}_e^{\text{ex}} x$$

with the y-intercept =  $\tilde{\nu}_e^{\text{ex}}$  and the x-intercept =  $v_{\text{cl}} + 1$ .

The exact result for the dissociation energy of the excited state is given by Eq. 28.2.15:  $\tilde{D}_0^{\text{ex}} = \frac{1}{2} \tilde{\nu}_e^{\text{ex}} v_{\text{cl}}$ . The dissociation energy is easily calculated exactly from the y-intercept and then  $v_{\text{cl}} = x\text{-intercept} - 1$ . This plot type is not commonly used, so we didn't cover it in the body of the chapter.

**25.** The ultra-violet photoelectron spectrum of HCl taken with He discharge excitation at 21.21 eV is shown below.<sup>7,8</sup> The doublet peaks at 12.74-12.82 and at 13.04-13.12 occur for the  $^2\Pi_{3/2}$  and  $^2\Pi_{1/2}$  states. The doublet spacing is determined by spin-orbit coupling. The peak spacings listed on the spectrum are vibrational spacings. The ground state spectroscopic constants for HCl are listed in Table 27.6.1. (a). For each band, is the molecular ion stretching frequency greater, roughly equal, or less than that of the ground state HCl? Predict the type of orbital, bonding, non-bonding, or anti-bonding, of the corresponding ionized electron. Include observations on the length of the vibrational progression of each band. (b). The molecular orbital diagram for HI is given in Figure 28.2.7. Is the molecular orbital ordering for HCl consistent with the molecular orbital ordering for HI?

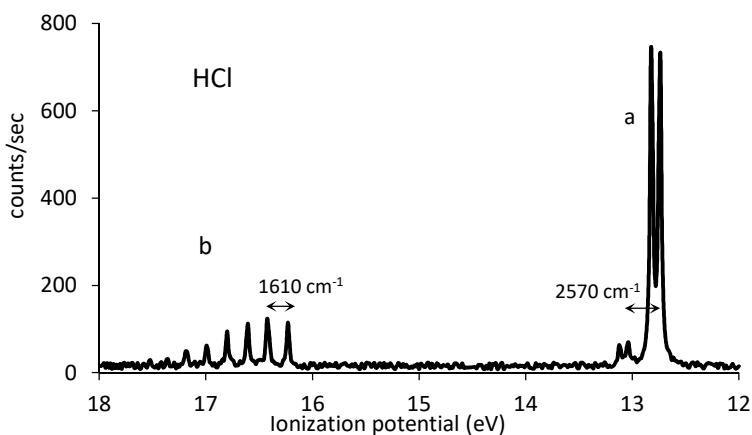


Figure 28.25.1: UPS spectrum of HCl using He discharge excitation at 21.21 eV.

*Answer:* The plan is to note that, for comparison, the observed fundamental vibration frequency for HCl is  $\tilde{\nu}_0 = \tilde{\nu}_e - 2\chi_e\tilde{\nu}_e = 2990.925 - 2(52.800) \text{ cm}^{-1} = 2885.325 \text{ cm}^{-1}$ , using Eq. 27.5.11.

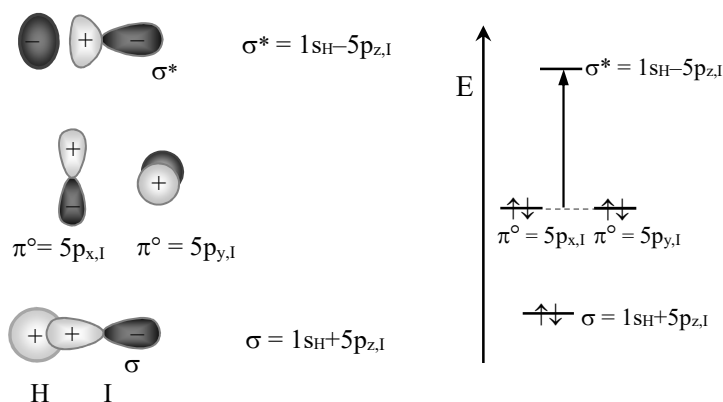
(a). The fundamental vibration frequency for the ground state of the molecular ion given for the a-band is only slightly smaller than the ground state, suggesting the removal of a non-bonding orbital. The removal of a high energy non-bonding electron is not surprising for halogens. The fundamental vibration frequency for the excited state of the molecular ion given for the b-band is significantly less than the ground state, suggesting the removal of a bonding electron.

The length of each vibrational progression is consistent with these observations. The vibrational fine-structure includes only two transitions for the a-band, suggesting a small change in bond length between the neutral molecule and the molecular ion. The removal of the corresponding electron makes a small difference in the bond strength. The removal of a non-bonding electron produces no change in the qualitative bond order. The vibrational fine-structure includes seven or eight transitions for the b-band, suggesting a large change in bond length between the neutral molecule and the molecular ion. The removal of the corresponding electron makes a large difference in the bond strength. This result suggests that the electron is removed from a bonding orbital resulting in a smaller qualitative bond order.

(b). The lowest ionization energy for the molecular orbital ordering in Figure 28.2.7 for HI corresponds to the removal of a non-bonding atomic p-electron. The next ionization energy corresponds to the removal of a  $\sigma$ -bonding electron. This order is identical to the character of the transitions in the UPS spectrum. So even though the valence shell for Cl-atoms is 3s-3p the character of the molecular orbital diagram is similar.

26. The molecular orbital diagram for HI is given in Figure 28.2.7. (a). Sketch the four molecular orbitals. (b). Compare the molecular orbitals to the molecular orbitals for LiH, Figure 26.3.4. Suggest the reason why the 5s-orbital on the I-atom doesn't participate in the molecular orbitals to a significant extent (at least at a qualitative level). (c). The molecular orbital ordering in Figure 28.2.7 is verified using UPS. Describe the vibrational fine-structure in the UPS spectrum that is expected for HI. That is for each of the three bands, is the molecular ion stretching frequency greater, roughly equal, or less than that of the ground state HI? Also, is each vibrational progression short or long? (d). Show the "box diagrams" for the  $^2P_{1/2}$  and  $^2P_{3/2}$  states of I-atoms. (e). Find the term symbols for the excited states of HI with configuration  $\sigma^2(\pi^0)^3(\sigma^*)^1$ . (f). Determine the possible projections of the total angular momentum for each term:  $\Omega = |\Lambda + \Sigma_s|$ .

*Answer:* (a). The four molecular orbitals are diagrammed below, based on the listed molecular orbitals: bonding  $\sigma = 1s_H + 5p_{z,I}$ , non-bonding pure atomic  $\pi^0 = 5p_{x,I}$  and  $\pi^0 = 5p_{y,I}$ , and anti-bonding  $\sigma^* = 1s_H - 5p_{z,I}$ .

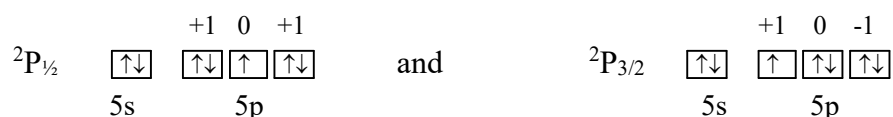


(b). For HI, the difference is the absence of the predominately non-bonding  $\sigma$ -orbital just below the purely non-bonding atomic p-orbitals. This non-bonding  $\sigma$ -orbital does not exist because the

5s orbital on the I-atom is so low in energy, relative to the 1s(H), that the 5s is core non-bonding. The unavailability of the 5s(I) leaves only two valence orbitals, the 1s(H) and the 2p(I) that points along the internuclear axis, to form the bonding and anti-bonding molecular orbitals.

(c). The UPS spectrum for HI has an appearance very similar to the spectrum of HCl, which is illustrated in the previous problem. Ionization from the HOMO, which is a non-bonding  $5p_x$  or  $5p_y$ , has little effect on the bond strength. The small change in bond strength predicts the lowest energy band to have a short vibrational progression and a molecular ion vibration frequency little changed from the neutral molecule. The next transition, transition-b in the previous problem, removes an electron from the strongly bonding  $\sigma$ -orbital, giving a large decrease in bond strength. As a result, the fundamental vibration frequency in the molecular ion is predicted to have a large decrease and a long vibrational progression.

(d). Schematically, representing each state with a single box diagram for the configuration  $[\text{Kr}]4d^{10}5s^25p^7$ :

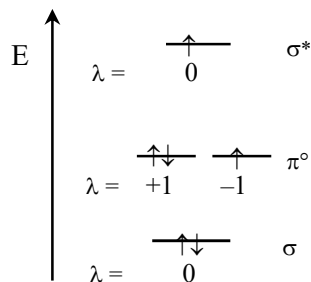


which represent the total angular momentum states given by the Clebsch-Gordan series:

$$\text{with } S = \frac{1}{2}, L = 1 \quad \text{then} \quad J: L-S, \dots, |L+S| = 1-\frac{1}{2}, 1+\frac{1}{2}$$

The atomic states have the overall degeneracies:  $g_J = 2$  for  ${}^2P_{1/2}$  and  $g_J = 2J+1 = 4$  for  ${}^2P_{3/2}$

(e). The term symbols for the molecular configuration  $\sigma^2(\pi^0)^3(\sigma^*)^1$  are given by adding the orbital angular momenta. The explicit configuration with maximum S and  $\Lambda$  is shown below, giving the total orbital angular momentum as  $\Lambda = 1$  for a  ${}^3\Pi$  term. The spin multiplicity can also be a singlet with paired spins giving a  ${}^1\Pi$  terms.



(f). For a  $\Pi$  state,  $\Lambda = 1$ . For the singlet  $S = \frac{1}{2}$  and for the triplet  $S = 1$ . The projection of the total angular momentum is given by the series.

For the singlet,  $S = \frac{1}{2}$ ,  $\Sigma_s = -\frac{1}{2}, +\frac{1}{2}$ ,  $\Lambda = 1$  with  $\Omega = |\Lambda + \Sigma_s| = \frac{1}{2}, \frac{3}{2}$   
giving  ${}^1\Pi_{1/2}$  and  ${}^1\Pi_{3/2}$  molecular terms.

For the triplet,  $S = 1$ ,  $\Sigma_s = -1, 0, +1$ ,  $\Lambda = 1$  with  $\Omega = |\Lambda + \Sigma_s| = 0, 1, 2$   
giving  ${}^3\Pi_0$ ,  ${}^3\Pi_1$ , and  ${}^3\Pi_2$  molecular terms.

Substates of the  ${}^1\Pi$  and the  ${}^3\Pi$  terms give the repulsive states diagramed in Figure 28.2.7b. The total angular momentum states for the transitions in HI are given in parentheses. The  ${}^3\Pi(0^+)$  state has  $\Omega = 0$  with the projection of the orbital angular momentum  $+\Lambda$ , rather than  $-\Lambda$  ( $\pm\Lambda$  states are

degenerate).<sup>4</sup> Note: Most authors use the symbol  $\Sigma$  and not  $\Sigma_s$  for the projection of the spin angular momentum. Unfortunately then, the two uses of the symbol  $\Sigma$ , which are the term symbol and the projection of the spin, must be distinguished by context.

27. Determine the density of states of a one-dimensional particle in a box. Determine the density of states near the state with quantum number  $n = 100$ , for  $\text{CO}_2$  molecules in a 10.0 cm “box”. Express the units as states per wave number.

*Answer:* The plan is to determine the derivative corresponding to Eq. 28.3.3, which is the derivative of the translational quantum number  $n$  with respect to the energy. The energy of the particle in a box states is given by given by Eq. 23.4.9.

The energy of a state with quantum number  $n$  is:  $E_n = \frac{h^2 n^2}{8ma^2}$  with a the box length.

$$\rho(\epsilon) = \frac{dn}{d\epsilon} = \left(\frac{d\epsilon}{dn}\right)^{-1} \quad \text{with} \quad \frac{d\epsilon}{dn} = \left(\frac{h^2}{8ma^2}\right) \frac{d n^2}{dn} = \left(\frac{h^2 n}{4ma^2}\right)$$

Substituting the derivative into the density of states gives:

$$\rho(\epsilon) = \frac{4ma^2}{h^2 n} \quad \text{states per joule}$$

For  $\text{CO}_2$  in a 10.0 cm box, for which  $m = 44.0 \text{ g mol}^{-1}/N_A/(1000 \text{ g/1 kg}) = 7.31 \times 10^{-26} \text{ kg}$ :

$$\rho(\epsilon) = \frac{4ma^2}{h^2 n} = \frac{4(7.31 \times 10^{-26} \text{ kg})(0.100 \text{ m})^2}{(6.626 \times 10^{-34} \text{ J s})^2 (100)} = 6.66 \times 10^{37} \text{ J}^{-1}$$

Remember that  $\tilde{E} = E/hc$  to convert to  $\text{cm}^{-1}$ . The density of states is per unit energy giving the conversion to wave numbers as:

$$\begin{aligned} \rho(\epsilon) &= 6.66 \times 10^{37} \text{ J}^{-1} (hc) = 6.66 \times 10^{37} \text{ J}^{-1} (6.626 \times 10^{-34} \text{ J s})(2.99792 \times 10^{10} \text{ cm s}^{-1}) \\ &= 1.32 \times 10^{15} \text{ cm} = 1.32 \times 10^{15} \frac{1}{\text{cm}^{-1}} \quad \text{that is } 1.32 \times 10^{15} \text{ states per wave number} \end{aligned}$$

The density of states decreases with increasing energy because the spacing between particle in a box energy levels increases with increasing  $n$ . However, even at  $n = 100$ , the density of states is amazingly high. We will find that for a 3-dimensional particle in a box, the density of states increases with increasing energy, because of degeneracy.

28. Determine the density of states of a linear rigid rotor. Rotational energy levels have a degeneracy of  $(2J + 1)$ , which we must take into account. The degeneracy is the number of states at a given energy level. The density of states is the product of the number of states at the given energy level with the number of levels per unit energy. The rotational constant for  $\text{H-C}\equiv\text{N}$  is  $1.4782 \text{ cm}^{-1}$ .<sup>9</sup> Calculate the density of states for  $\text{H-C}\equiv\text{N}$ .

*Answer:* The plan is to determine the derivative corresponding to Eq. 28.3.3, which is the derivative of the rotational quantum numbers  $J$  with respect to the energy, which is then multiplied by the degeneracy. The energy of the rotational states is given by given by Eq. 27.4.1.

The energy of a state with quantum number  $J$  is  $\epsilon_J = \tilde{B}hc J(J + 1)$  :

$$\rho(\epsilon) = (2J + 1) \frac{dJ}{d\epsilon} = (2J + 1) \left( \frac{d\epsilon}{dJ} \right)^{-1} \quad \text{with} \quad \frac{d\epsilon}{dJ} = \frac{d [\tilde{B}hc J(J + 1)]}{dJ} = \tilde{B}hc (2J + 1)$$

Substituting the derivative into the density of states gives:

$$\rho(\epsilon) = (2J + 1) [\tilde{B}hc (2J + 1)]^{-1} = \frac{1}{\tilde{B}hc} \quad \text{per joule} \quad \text{or} \quad \rho(\epsilon) = \frac{1}{\tilde{B}} \quad \text{per cm}^{-1}$$

The energy spacing between rotational levels increases with  $J$ , so we might expect the density of states decrease to increase with energy. However, the degeneracy increases with  $J$ . As a result the rotational density of states is constant with increasing energy. The rotational constant for  $\text{H-C}\equiv\text{N}$  is  $1.4782 \text{ cm}^{-1}$ .<sup>9</sup> The density of rotational states is  $\rho(\epsilon) = 1/1.4782 \text{ cm}^{-1} = 0.676 \text{ states per wave number}$ .

29. The UV-visible absorption spectrum of  $\text{SO}_2$  is given in Figure 28.1.1. The band origin of the visible transition is roughly 340 nm. The band origin corresponds to the  $\nu' \leftarrow \nu''$  vibrational fine-structure transition of  $0 \leftarrow 0$ . Consider non-radiative energy transfer by internal conversion from this excited electronic state into the ground electronic state. The three normal modes of  $\text{SO}_2$  in the ground electronic state are at wave numbers  $1151 \text{ cm}^{-1}$ ,  $518 \text{ cm}^{-1}$ , and  $1362 \text{ cm}^{-1}$ , Figure 28.3.2. (a) Assuming all the vibrational energy is in the asymmetric stretch- $\nu_3$ , that is  $\nu_1 = \nu_2 = 0$ , calculate the vibrational quantum number of the ground state that is isoenergetic with the lowest energy vibrational level of the excited state. (b). Assuming the vibrational quantum numbers are all equal, that is  $\nu_1 = \nu_2 = \nu_3$ , calculate the approximate vibrational quantum numbers of the ground state that is isoenergetic with the lowest energy vibrational level of the excited state.

*Answer:* The plan is to convert the band origin to wave numbers and then compare with the harmonic oscillator energy levels.

In wave numbers,  $\tilde{\nu}_{00} = [1/(340 \times 10^{-9} \text{ m})] (1 \text{ m}/100 \text{ cm}) = 29400 \text{ cm}^{-1}$ . This energy is referenced to the zero-point energy of the ground state at  $\tilde{G}(0) = \frac{1}{2}\tilde{\nu}_0$ .

(a). Using the energy of a harmonic oscillator as  $\tilde{G}(\nu) = \tilde{\nu}_0(\nu + \frac{1}{2})$  gives:  $\nu = \tilde{\nu}_{00}/\tilde{\nu}_0 = 29400 \text{ cm}^{-1}/1362 \text{ cm}^{-1} = 21.6 \cong 22$ . This is a highly excited vibrational level, which may be near the dissociation limit.

(b). What happens if we don't put all our eggs in one basket and consider vibrational excitation into each of the normal modes?

$$\nu = \frac{\tilde{\nu}_{00}}{(\tilde{\nu}_{1,0} + \tilde{\nu}_{2,0} + \tilde{\nu}_{3,0})} = \frac{29400 \text{ cm}^{-1}}{1151 \text{ cm}^{-1} + 518 \text{ cm}^{-1} + 1362 \text{ cm}^{-1}} = 9.70 \cong 10$$

This vibrational level is very difficult to access using absorption directly from the ground electronic state (by infrared absorption spectroscopy for example). However, internal conversion

is seen to be mediated through such highly excited vibrational states. We assumed that all the vibrational quantum numbers were equal. However, a given molecular system may prefer to have more quanta in the modes with higher fundamental vibration frequency. For example, very high frequency C–H stretching vibrations play an important role in internal conversion processes in aromatic systems.

**30.** Avoided-crossings of degenerate states follow a common pattern. Consider two states represented by the wave functions  $\Psi_A$  and  $\Psi_B$ . The strength of the interaction between the two states is determined by the integral  $c = \int \Psi_A \hat{o} \Psi_B d\tau$ . Possibilities for the  $\hat{o}$  operator include spin-orbit coupling for electronic interactions in intersystem crossing or  $(\partial^2/\partial R^2)$  for vibronically coupled states. Vibronic coupling is important in internal conversion and pre-dissociation. We consider the interaction as a perturbation on the unperturbed wave functions  $\Psi_A$  and  $\Psi_B$ . We assume that there is no net interaction without the perturbation, giving an overlap-type integral:

$$\int \Psi_A \Psi_B d\tau = S_{AB} = 0$$

A zero overlap integral is often the result of orthogonality. Any two different electronic states of the same molecule are orthogonal. The unperturbed energies of the two states are:

$$a = \int \Psi_A \hat{H}' \Psi_A d\tau \quad \text{and} \quad b = \int \Psi_B \hat{H}' \Psi_B d\tau$$

with  $\hat{H}'$  given by the unperturbed Hamiltonian ( $\hat{o}$  is not present). The energies of the two states with the interaction present are the eigenvalues of the secular equations,  $\lambda_i$ , as in Eq. 26.1.13:

$$\begin{vmatrix} a - \lambda & c \\ c & b - \lambda \end{vmatrix} = 0$$

with the eigenvalues given by Eq. 6.3.23. Recasting Eq. 6.3.23 into the terms used in this problem gives:

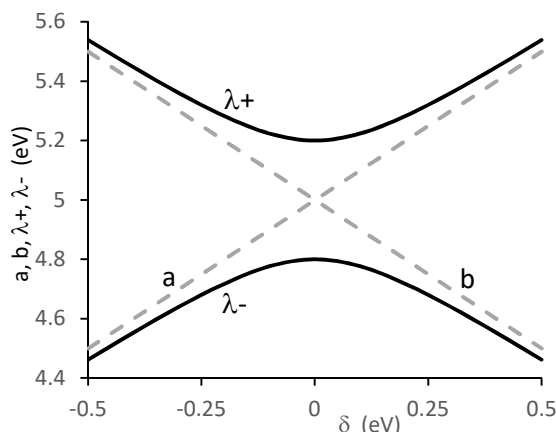
$$\lambda_i = \frac{(a + b) \pm \sqrt{(a - b)^2 + 4 c^2}}{2} \quad \text{P28.32.1}$$

- (a). In pre-dissociation,  $a$  and  $b$  scale with the distance, with  $a = b$  at the avoided-crossing. Assume the two states are nearly degenerate and have energies:  $a = 5.00 \text{ eV} + \delta$  and  $b = 5.00 \text{ eV} - \delta$ . The energy gap,  $\delta$ , has units of eV. Plot the energies of the two states with the interaction present for  $c = 0.2 \text{ eV}$  for  $\delta$  in the range of  $-0.5 < \delta < 0.5$ . Determine the energy gap at  $\delta = 0$ .
- (b). Compare the previous plot to Figure 28.2.8. How can you tell that the crossing is avoided?
- (c). Decrease the interaction parameter to  $c = 0.01 \text{ eV}$ . Is the interaction still avoided? RT at room temperature is  $0.0257 \text{ eV}$ . Predict the behavior of the system at room temperature at the avoided-crossing.

*Answer:* The plan is to solve for the eigenvalues as a function of the energy gap,  $\delta$ . For large positive energy gaps,  $\lambda_+ \cong a$  and  $\lambda_- \cong b$ .

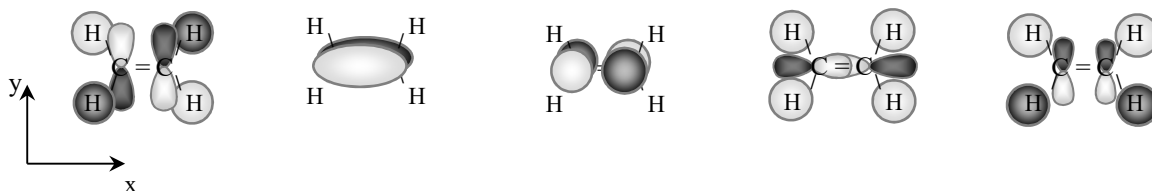
A spreadsheet was developed that solves P28.32.1 as a function of the energy gap parameter.

A1	B	C	D	E	F	G	
2		$E_{av} =$	5	eV	$c =$	0.2	eV
3		$\delta$	a	b	$\lambda_+$	$\lambda_-$	
4		-0.5	4.5	5.5	5.5385	4.4615	
5		-0.4	4.6	5.4	5.4472	4.5528	
6		-0.3	4.7	5.3	5.3606	4.6394	
7		-0.2	4.8	5.2	5.2828	4.7172	
8		-0.1	4.9	5.1	5.2236	4.7764	
9		0	5	5	5.2000	4.8000	
10		0.1	5.1	4.9	5.2236	4.7764	
11		0.2	5.2	4.8	5.2828	4.7172	
12		0.3	5.3	4.7	5.3606	4.6394	
13		0.4	5.4	4.6	5.4472	4.5528	
14		0.5	5.5	4.5	5.5385	4.4615	



- (a). The energy gap at the curve-crossing is  $0.4 \text{ eV} = 2c$ .
- (b). The curve is analogous to pre-dissociation assuming a linear change in unperturbed energy with distance, near the curve-crossing. You can tell that the crossing is avoided because the  $\lambda_+$  curve approaches curve-b for negative energy gaps, but approaches curve-a for positive energy gaps. If the system starts in the a-state, for increasing  $\delta$  the system progresses to the b-state for large  $\delta$ .
- (c). Decreasing the interaction parameter decreases the gap at the curve-crossing. If  $c = 0.01 \text{ eV}$ , the gap is only  $0.02 \text{ eV}$  at the avoided-crossing. This gap is smaller than the available thermal kinetic energy, which easily allows the system to jump across the gap. As a consequence if the system starts in the a-state, for increasing  $\delta$  at the curve crossing the system can jump to the upper curve. Then instead of progressing to the b-state for large  $\delta$ , the system stays in the a-state. The result is a mixture of products, some in the a-state and some in the b-state.

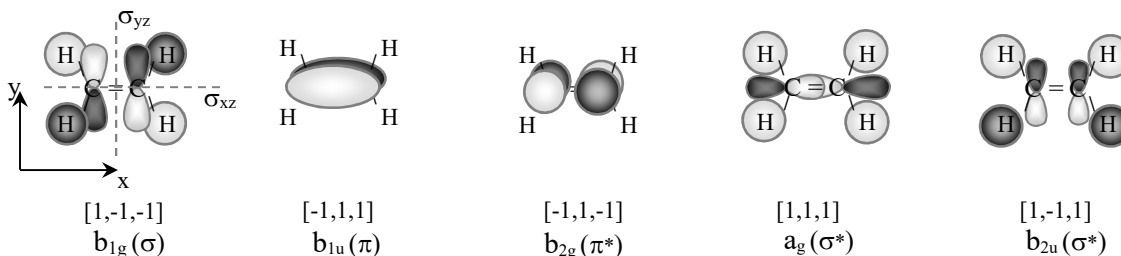
31. Determine the symmetry species of the following molecular orbitals of ethylene. The symmetry species are the irreducible representations. In addition, classify the molecular orbitals as  $\sigma$  or  $\pi$ , non-bonding or bonding.



*Answer:* The plan is to note that the point group is  $D_{2h}$  for ethylene. The sufficient characteristic symmetries are the transformation properties under  $\sigma(xy)$ ,  $\sigma(xz)$ , and  $\sigma(yz)$ .

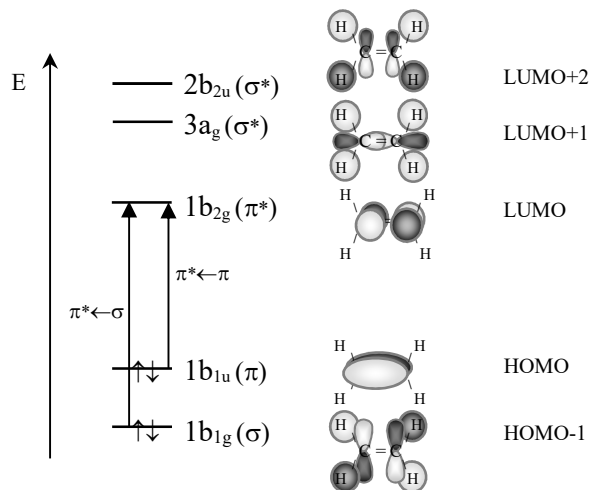
We don't need to consider every symmetry operation of the point group. Such a complete enumeration could drive you crazy with some of the more symmetrical point groups. We can use just  $\sigma(xy)$ ,  $\sigma(xz)$ , and  $\sigma(yz)$  since the results are unique and easy to see. The  $\sigma(xy)$ -plane contains all the atoms. For example, the first molecular orbital is symmetric with respect to the  $\sigma(xy)$ -plane, antisymmetric with respect to  $\sigma(xz)$ , and antisymmetric with respect to  $\sigma(yz)$ . Symbolizing symmetric with +1 and antisymmetric with -1, the results in the order

$[\sigma(xy), \sigma(xz), \sigma(yz)]$  are  $[1, -1, -1]$ . Comparison with the  $D_{2h}$  character table shows these characters correspond to  $B_{1g}$ . The orbital overlaps are all in-plane and correspond to C–H bonds, giving a  $\sigma$ -type orbital. The molecular orbital has four bonding C–H interactions and one anti-bonding C–C interaction, which is net bonding. The other results are given below.



We can check our results by noting the transformation properties under inversion. The symmetric orbitals under inversion are g and the anti-symmetric orbitals are u, which agrees with our assignments. The choice of the  $\sigma(xy)$ ,  $\sigma(xz)$ , and  $\sigma(yz)$  planes is in some ways arbitrary; other combinations of transformations also work. However, usually reflection planes are often the most convenient as long as the results give a unique one-to-one relationship with the irreducible representations of the point group.

**32.** Use electronic selection rules to determine if the LUMO+1  $\leftarrow$  HOMO and LUMO+2  $\leftarrow$  HOMO transition are allowed in absorption spectra. The corresponding molecular orbital diagram for the  $1b_{1g}$ ,  $1b_{1u}$ ,  $1b_{2g}$ ,  $a_g$ , and  $b_{2g}$  levels is given below.



*Answer:* The plan is to determine the direct products  $A_{1g} \otimes B_{1u}$  and  $B_{2u} \otimes B_{1u}$ .

The ground electronic state for ethylene is  $A_{1g}$ , since all occupied orbitals are doubly filled. As a result we need only consider the symmetry of the excited state and the electric dipole operator. In  $D_{2h}$  the x, y, and z components of the electric dipole transform as  $B_3$ ,  $B_2$ , and  $B_1$ , respectively. The LUMO+1  $\leftarrow$  HOMO transition gives an excited state with configuration  $\dots(1b_{1g})^2(1b_{1u})^1(1b_{2g})^0(a_g)^1$  with direct product:  $A_{1g} \otimes B_{1u}$ . The  $A_{1g}$  irreducible representation is the totally symmetric representation. Multiplication by the totally symmetric representation is the

unity operation for direct products, since all the characters are +1. As a result  $A_{1g} \otimes B_{1u} = B_{1u}$ . The z-component of the dipole moment transforms as  $B_{1u}$ , which gives the transition as allowed for the singlet states:  ${}^1B_{1u} \leftarrow {}^1A_{1g}$ .

The LUMO+2  $\leftarrow$  HOMO transition gives an excited state with configuration  $\dots(1b_{1g})^2(1b_{1u})^1(1b_{2g})^0(a_g)^1(2b_{2u})^1$  with direct product:  $B_{2u} \otimes B_{1u}$ . We can save ourselves some time by noting that the direct product will have g-parity. The x, y, and z-components of the dipole moment transform as u-parity, which gives the transition as forbidden. However, for practice, the direct product  $B_{2u} \otimes B_{1u}$  is:

$D_{2h}$	E	$C_2(z)$	$C_2(y)$	$C_2(x)$	$i$	$\sigma(xy)$	$\sigma(xz)$	$\sigma(yz)$
$B_{1u}$	1	1	-1	-1	-1	-1	1	1
$B_{2u}$	1	-1	1	-1	-1	1	-1	1
$B_{2u} \otimes B_{1u}$	1	-1	-1	1	1	-1	-1	$1 = B_{3g}$

The result has g-parity as predicted giving a forbidden transition. The next problem gives the result from an electronic structure calculation using CIS/6-311G\*, which agrees with the results in this problem. However, it is found that the LUMO+1  $\leftarrow$  HOMO transition, which is  ${}^1B_{1u} \leftarrow {}^1A_{1g}$ , while allowed is significantly less intense than the LUMO  $\leftarrow$  HOMO transition.

33. In Example 28.8.1 we used group theory based electronic selection rules to determine if the low energy  $\pi^* \leftarrow \sigma$  and  $\pi^* \leftarrow \pi$  transitions of ethylene are allowed or forbidden. Configuration interaction calculations are used to find excited states, electronic transition energies, and intensities within the Hartree-Fock formalism. Single excitations don't contribute to ground state stability, however single excitations generate many possible excited states. As a consequence configuration interaction with single excitations, CIS, is used to simulate UV-visible spectra. First, do a geometry optimization for ethylene at HF/6-311G\* (equivalent to HF/6-311G(d)). Then do a CIS/6-311G\* single point calculation to compare to the intensity predictions in Example 28.8.1. [Hints: To do a CIS calculation: Using the [Spartan](#) visualization environment select an Energy calculation and check "UV/Vis" and "Orbitals & Energies". Using the [WebMo](#) visualization environment for Gaussian choose the Calculation type as "Excited States and UV-Vis". Use the Basis Set "Other" option to specify 6-311G(d). Using the [GaussView](#) visualization environment for Gaussian set the Method as CIS and check "Solve for More States, N = 6".]

*Answer:* We give the Spartan version first and then the Gaussian version. The Spartan/Q-Chem results are shown below with transition wavelengths in nm:

```
UV/Vis Allowed Transitions:
nm   strength MO Component
115.69 0.0000 HOMO-2 -> LUMO 92%
125.52 0.0000 HOMO -> LUMO+3 95%
128.17 0.0000 HOMO-1 -> LUMO 92%
135.48 0.0000 HOMO -> LUMO+2 89%
142.34 0.0443 HOMO -> LUMO+1 99%
146.10 0.6127 HOMO -> LUMO 94%
```

In Example 28.8.1, we predicted the LUMO  $\leftarrow$  HOMO transition to be fully allowed with  $B_{3u}$  symmetry and the LUMO  $\leftarrow$  HOMO-1 transition to be forbidden with  $B_{3g}$  symmetry. The CIS results agree with the group theory predictions. The calculation places the LUMO+1  $\leftarrow$  HOMO

transition that is weakly allowed and the LUMO+2←HOMO forbidden transition in between the transitions in Example 28.8.1.

The Gaussian results at CIS(NStates=10)/6-311G(d), as displayed by the WebMo “front-end” visualization environment, are shown below with transition wavelengths in nm.

State	Symmetry	Energy (nm)
1	B1U	146.05
2	B3U	142.28
3	B1G	135.45
4	B1G	128.18
5	B2G	125.49
6	B2G	115.61
7	AU	106.02
8	B3G	104.97
9	B2U	96.32
10	AU	95.40

A plot of the electronic spectrum shows only the first transition, B1U at 146.05 nm, has significant intensity. We need to view the “raw” numerical data file to determine the molecular orbitals involved in the transition. Ethylene has 16 electrons, so that the HOMO is orbital 8. The orbitals are listed with the molecular orbital symmetry designations as:

```

Occupied (AG) (B1U) (AG) (B1U) (B2U) (AG) (B3G) (B3U)
Virtual  (B2G) (AG) (B2U) (B1U) (B3G) (B1U) (AG) (B2U)
          (AG) (B3U) (B1U) (B2G) (B2U) (B3G) (AG) (B1U)
          (B3G) (B1U) (B1G) (B3U) (B2U) (AG) (AU) (B1U)
          (AG) (B3G) (B2G) (AG) (B1U) (B2U) (B1U) (B3U)
          (B3G) (B2G) (B2U) (AG) (B3G) (B1U) (AG) (B1U)

```

Comparison of the assigned molecular orbital symmetries to Figure 28.8.2 shows the designations of the B<sub>1</sub> and B<sub>3</sub> molecular orbital labels to be switched. Unfortunately there is no definitive choice of symmetry labels for B<sub>1</sub>, B<sub>2</sub>, and B<sub>3</sub>; different authors use different labels. We just need to remember the switch when comparing to our original molecular orbital diagram.

The spectroscopic transitions are listed below.

Excitation energies and oscillator strengths:

```

Excited State 1: Singlet-B1U      8.4892 eV  146.05 nm  f=0.6131
      8 -> 9      0.68385
This state for optimization and/or second-order correction.
Copying the excited state density for this state as the 1-particle RhoCI density.

Excited State 2: Singlet-B3U      8.7144 eV  142.28 nm  f=0.0444
      8 -> 10     0.70271

Excited State 3: Singlet-B1G      9.1537 eV  135.45 nm  f=0.0000
      7 -> 9      0.18364
      8 -> 11     0.66646
      8 -> 16     0.11486

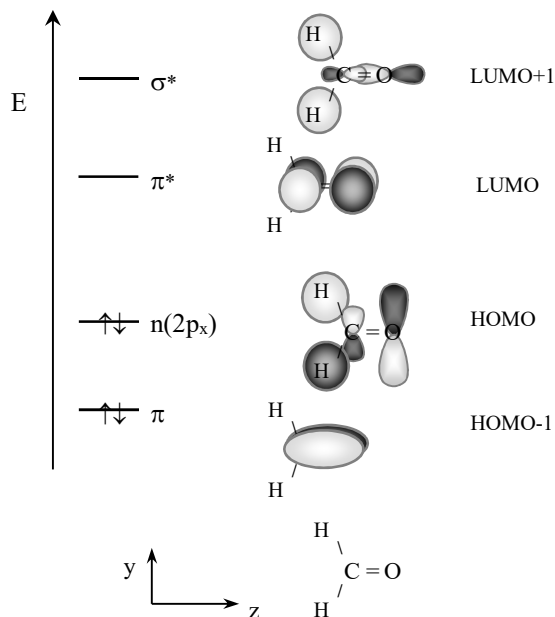
Excited State 4: Singlet-B1G      9.6728 eV  128.18 nm  f=0.0000
      7 -> 9      0.67617
      8 -> 11     -0.18519

```

The LUMO←HOMO transition corresponds to orbitals 8 → 9 in the listings, below. The LUMO+2←HOMO transition corresponds to 8 → 11, which is the largest contributor to transition 3. In Example 28.8.1, we predicted the LUMO←HOMO transition to be fully allowed with B<sub>2g</sub>⊗B<sub>1u</sub> = B<sub>3u</sub> symmetry and the LUMO←HOMO-1 transition to be forbidden with B<sub>2g</sub>⊗B<sub>1g</sub> = B<sub>3g</sub> symmetry. Given the switch in labels, the CIS results agree as listed below for

transitions 1 and 4. The calculation interposes transition 2, the LUMO+1 $\leftarrow$ HOMO transition as weakly allowed, and transition 3, the LUMO+2 $\leftarrow$ HOMO transition as forbidden.

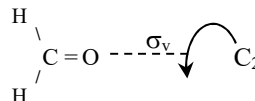
34. Determine the symmetry species of the following molecular orbitals of formaldehyde. The geometry is shown at bottom. The x-direction is the  $\pi$ -bonding direction for these plots. The HOMO has a small contribution from the  $2p_y$  orbital on the C-atom. As a result the HOMO is primarily a non-bonding  $2p_y$  atomic orbital on the O-atom. [Hint: Use the symmetry operations given in Figure 26.6.4. Formal group theory is not required for this problem.]



*Answer:* The plan is to orient the  $C_2$  axis along  $z$  and the  $\sigma_v$ -plane along the  $z$ - and  $x$ -axes. The atoms then lie on the  $z$ - $y$  plane, which is called the  $\sigma_v'$ -plane.

The symmetry operations are given in Figure 26.6.4 and reproduced below:

symmetry	rotate $180^\circ$ ( $C_2$ )	reflect across $\sigma_v$
symmetric	a	1
antisymmetric	b	2



The HOMO-1 is antisymmetric with respect to  $180^\circ$  rotation and symmetric with respect to reflection across  $\sigma_v$ . The HOMO-1 has  $b_1$  symmetry.

The HOMO is antisymmetric with respect to  $180^\circ$  rotation and antisymmetric with respect to reflection across  $\sigma_v$ . The HOMO-1 has  $b_2$  symmetry.

The LUMO is antisymmetric with respect to  $180^\circ$  rotation and symmetric with respect to reflection across  $\sigma_v$ . The LUMO has  $b_1$  symmetry.

The LUMO+1 is symmetric with respect to  $180^\circ$  rotation and symmetric with respect to reflection across  $\sigma_v$ . The LUMO has  $a_1$  symmetry.

These symmetry designations are applied in the next problem.

35. Use electronic selection rules to determine if the LUMO←HOMO, LUMO←HOMO-1, and LUMO+1←HOMO electronic transitions of formaldehyde are allowed or forbidden. The symmetries of the molecular orbitals are:

Orbital	7	8	9	10
MO	HOMO-1	HOMO	LUMO	LUMO+1
Symmetry	b <sub>1</sub>	b <sub>2</sub>	b <sub>1</sub>	a <sub>1</sub>
Type	π	n	π*	σ*

*Answer:* The plan is to follow Example 28.8.1 under the C<sub>2v</sub> point group.

The ground electronic state for formaldehyde is A<sub>1</sub>, since all occupied orbitals are doubly filled. As a result we need only consider the symmetry of the excited state and the electric dipole operator. In C<sub>2v</sub> the x, y, and z components of the electric dipole transform as B<sub>2</sub>, B<sub>1</sub> and A<sub>1</sub>. The required direct products of the upper and lower singly occupied molecular orbitals in the excited state are:

LUMO←HOMO with orbital types π\*←n gives excited electronic state configuration

...(b<sub>1</sub>)<sup>2</sup>(b<sub>2</sub>)<sup>1</sup>(b<sub>1</sub>)<sup>1</sup> with symmetry B<sub>1</sub>⊗B<sub>2</sub> :

MO Symmetry	E	C <sub>2</sub>	σ <sub>v</sub>	σ <sub>v</sub> '	Result
B <sub>1</sub>	1	-1	1	-1	
B <sub>2</sub>	1	-1	-1	1	
B <sub>1</sub> ⊗B <sub>2</sub>	1	1	-1	-1	= A <sub>2</sub> <b>forbidden</b>

The A<sub>2</sub> symmetry of the excited state does not match a component of the electric dipole moment, giving a forbidden transition.

LUMO←HOMO-1 with orbital types π\*←σ gives excited electronic state configuration

...(b<sub>1</sub>)<sup>1</sup>(b<sub>2</sub>)<sup>2</sup>(b<sub>1</sub>)<sup>1</sup> symmetry B<sub>1</sub>⊗B<sub>1</sub> :

MO Symmetry	E	C <sub>2</sub>	σ <sub>v</sub>	σ <sub>v</sub> '	Result
B <sub>1</sub>	1	-1	1	-1	
B <sub>2</sub>	1	-1	1	-1	
B <sub>1</sub> ⊗B <sub>2</sub>	1	1	1	1	= A <sub>1</sub> <b>allowed</b>

The A<sub>1</sub> symmetry of the excited state matches the z-component of the electric dipole moment, giving an allowed transition. We could have saved ourselves some work since the product of any non-degenerate irreducible representation with itself is always the totally symmetric group.

LUMO+1←HOMO with orbital types σ\*←σ gives excited electronic state configuration

...(b<sub>1</sub>)<sup>2</sup>(b<sub>2</sub>)<sup>2</sup>(b<sub>1</sub>)<sup>0</sup>(a<sub>1</sub>)<sup>1</sup> symmetry A<sub>1</sub>⊗B<sub>2</sub> = B<sub>2</sub>. The A<sub>1</sub> irreducible representation is the totally symmetric representation. Multiplication by the totally symmetric representation is the unity operation for direct products, since all the characters are +1. As a result A<sub>1</sub>⊗B<sub>2</sub> = B<sub>2</sub>. The B<sub>2</sub> symmetry of the excited state matches the y-component of the electric dipole moment, giving an **allowed** transition. The next problem gives the result from an electronic structure calculation using CIS/6-311G\*, which agrees with the results in this problem.

36. Use a configuration interaction-singles calculation to determine the predicted intensity of the LUMO←HOMO, LUMO←HOMO-1, and LUMO+1←HOMO electronic transitions of formaldehyde. First, do a geometry optimization for formaldehyde at HF/6-311G\*\* (equivalent to HF/6-311G(d,p)). Then do a CIS/6-311G\*\* single point calculation to compare to the intensity predictions in Problem 35. See Problem 33 for a discussion of the use of CIS calculations for predicting electronic spectra and for hints on doing the calculations.

*Answer:* All spin allowed transitions are for the singlet states, since the ground state of formaldehyde is a singlet,  $^1A_1$ . We give the Spartan version first and then the Gaussian version. The Spartan/Q-Chem results are:

```
UV/Vis Allowed Transitions:
nm strength MO Component
103.83 0.0000 HOMO-3 -> LUMO 95%
104.28 0.3556 HOMO -> LUMO+2 90%
117.65 0.1685 HOMO-1 -> LUMO 83%
120.16 0.0006 HOMO-2 -> LUMO 96%
125.60 0.1762 HOMO -> LUMO+1 97%
261.24 0.0000 HOMO -> LUMO 96%
```

The Gaussian results at CIS/6-311G(d), as displayed by the WebMo “front-end” visualization environment, are shown below with transition wavelengths in nm.

State	Symmetry	Energy (nm)
1	A2	261.26
2	B2	125.58
3	B1	120.17
4	A1	117.65
5	A1	104.28
6	A2	103.82
7	B2	99.65
8	B1	95.52
9	A2	86.78
10	B1	80.14

We need to view the “raw” Gaussian numerical data file to determine the molecular orbitals involved in the transition. Formaldehyde has 16 electrons, so that the HOMO is orbital 8. The orbitals are listed with the molecular orbital symmetry designations as:

```
Orbital symmetries:
Occupied (A1) (A1) (A1) (A1) (B2) (A1) (B1) (B2)
Virtual (B1) (A1) (B2) (A1) (A1) (B2) (B1) (B2) (A1) (A1)
(A1) (B1) (B2) (A2) (B1) (A1) (A1) (B2) (B2) (A1)
(B1) (A2) (A1) (B2) (B2) (A1) (A1) (B1) (A2) (A1)
(B1) (A1) (B2) (B2) (A1) (B1) (B2) (A1) (A1) (A1)
```

The orbital symmetry labels, that is B<sub>1</sub> versus B<sub>2</sub>, match those given in Problem 35. The B<sub>1</sub> and B<sub>2</sub> designations are arbitrary and don't necessarily match.

The spectroscopic transitions are listed below.

Excitation energies and oscillator strengths:

```
Excited State 1: Singlet-A2 4.7456 eV 261.26 nm f=0.0000
8 -> 9 0.69294
```

This state for optimization and/or second-order correction.

Copying the excited state density for this state as the 1-particle RhoCI density.

Excited State	2:	Singlet-B2	9.8726 eV	125.58 nm	f=0.1760
8 -> 10		0.69548			
Excited State	3:	Singlet-B1	10.3177 eV	120.17 nm	f=0.0006
6 -> 9		0.69272			
Excited State	4:	Singlet-A1	10.5388 eV	117.65 nm	f=0.1688
7 -> 9		0.64570			
8 -> 11		0.19390			
8 -> 14		-0.13077			
Excited State	5:	Singlet-A1	11.8893 eV	104.28 nm	f=0.3552
7 -> 9		-0.17516			
8 -> 11		0.67138			

The LUMO←HOMO transition is for orbitals 8 -> 9, which has zero oscillator strength corresponding to a forbidden transition. The LUMO←HOMO-1 transition is for orbitals 7 -> 9, which is the largest contributor to transition 4. Transition 4 is allowed. The LUMO+1←HOMO transition corresponds to 8 -> 10, which is transition 2. Transition 2 is allowed. The CIS results agree as listed below for transitions 1 and 4. The calculation interposes transition 3, 6 -> 9 LUMO←HOMO-2 transition, as very weakly allowed.

Comparison with experimental spectra don't work out well for formaldehyde. The LUMO+1←HOMO, LUMO←HOMO-1, and LUMO←HOMO-2 transitions are not observed. A series of O-atom centered Rydberg transitions is prominent in the spectrum. One reason for the disagreement is that the  $^1A_2$  and  $^3A_2$  excited states are not planar, which these calculations do not take into account. The point group of these excited states is  $C_s$ .<sup>10</sup> Careful geometry optimized calculations on the excited states at higher levels than CIS are required to completely understand the spectra of many molecules, formaldehyde included. However, CIS calculations are a reasonable starting point, at least as a point of comparison.

37. K. P. Huber and G. Herzberg have produced a comprehensive reference on the spectroscopic data of diatomic molecules.<sup>3</sup> This reference has been transcribed by the National Institute of Standards and Technology, NIST, as an on-line database.<sup>2</sup> The entry for Na<sub>2</sub> is listed as an example below. The spectroscopic constants are presented in wave numbers and the equilibrium bond length in Å. The book tables start with a listing of the reduced mass,  $\mu$ , in g mol<sup>-1</sup>. Next the dissociation energy at absolute zero,  $D_0^o$ , which we have been referencing as just  $D_0$ , and the ionization energy to form the ground state of the molecular ion, I.P. The on-line version excludes  $\mu$ ,  $D_0^o$ , and I.P. By convention, the ground state is labeled as X, which for Na<sub>2</sub> is explicitly X  $^1\Sigma_g^+$ . Excited electronic states are labeled as states A, B, C, D ... in order of increasing energy if the states have the same spin multiplicity, or a, b, c, d ... if the excited states have a different multiplicity. Many literature references and many notes are included in the tables, which we have omitted in this example for brevity. For this homework problem (a) find the Na<sub>2</sub> reference in the book or on-line, <http://webbook.nist.gov/chemistry>, and (b) write a spreadsheet to plot the potential energy surfaces as a function of R for the X ground state, and A and B excited states. Use the Morse function for the potential energy surfaces. The A and B excited states dissociate to a ground and excited state Na atom: Na<sub>2</sub> → Na ( $^2S$ ) + Na ( $^2P$ ). The atomic excitation energy,  $\Delta E_{\text{atomic}}$  is 16961 cm<sup>-1</sup> to the  $^2P_{1/2}$  state. From Figure 28.2.5, note that  $\tilde{T}_e + \tilde{D}_e^{\text{ex}} = \tilde{D}_e + \Delta E_{\text{atomic}}$ .

State (1)	$T_e$	$\omega_e$	$\omega_e \chi_e$	$\omega_e y_e$	$B_e$ (2)	$\alpha_e$	$D_e$ (3)	$r_e$	Trans.	$v_{00}$
$^{23}\text{Na}_2$	$\mu = 11.4948852$		$D_8^g = 0.720 \text{ eV}^a$		$\text{I.P.} = 4.90 \text{ eV}^b$					
	Diffuse bands of $\text{Na}_2$ Van der Waals molecules close to the lines of principal series of Na.									
	Several fragments of other UV emission and absorption band systems. <sup>c</sup>									
E ( $^1\Pi_u$ )	35557	106.2 <sup>H</sup>	0.65						E $\leftarrow$ X R	35530.6 <sup>H</sup>
D ( $^1\Pi_u$ )	33486.8	111.3 <sup>H</sup>	0.48		d				D $\leftrightarrow$ X R	33462.9 <sup>H</sup>
$^1\Sigma_g^+$	(33000)	Fragment observed in two-photon excited $\text{Na}_2$ fluorescence								
C ( $^1\Pi_u$ )	29382	119.33 <sup>H</sup>	0.53		d				C $\leftrightarrow$ X R	29362 <sup>H</sup>
B ( $^1\Pi_u$ )	20320.02	124.090 <sup>Z</sup>	0.6999		0.125277	7.237E-4	3.248E-7	3.4228	B $\leftrightarrow$ X R	20302.49 <sup>Z</sup>
A ( $^1\Sigma_u^+$ )	14680.58	117.323 <sup>Z</sup>	0.3576		0.110784	5.488E-4	3.882E-7	3.6384	A $\leftrightarrow$ X R	14659.80 <sup>Z</sup>
a ( $^3\Pi_v$ )	<14680	(145)			(0.140)					
X ( $^1\Sigma_g^+$ )	0	159.1245 <sup>Z</sup>	0.72547		0.154707	8.736E-4	5.811E-7	3.07887		

a. From  $D_8^g = 5890 \pm 70 \text{ cm}^{-1}$  based on RKR potential curve for the ground state. The thermochemical value obtained by a molecular beam technique is 0.732 eV.

b. From photoionization. A similar value is obtained by extrapolation of the Rydberg series B, C, D, E.

c. Molecular absorption cross sections 27000 – 625000  $\text{cm}^{-1}$ .

d. Barrow, Travis, et al., 1960 report the following rotational constants for D:  $B_e = 0.1185$ ,  $\alpha_e = 0.001$ , C:  $B_e = 0.12815$ ,  $\alpha_e = 0.00084$ . Considerably different constants, however, are quoted by Richards in Rosen, 1970. D:  $B_e = 0.1152$ ,  $\alpha_e = 0.00110$ , C:  $B_e = 0.1185$ ,  $\alpha_e = 0.00096$ .

#### Footnotes:

1. Units:  $T_e$ ,  $\omega_e$ ,  $\omega_e \chi_e$ ,  $\omega_e y_e$ ,  $B_e$ ,  $\alpha_e$ ,  $D_e$ , and  $v_{00}$  in  $\text{cm}^{-1}$ , with  $\omega_e = \tilde{\nu}_e$  and  $r_e = R_e$  in  $\text{\AA}$  as given in this text.

2. On-line NIST tables list the vibration-rotation interaction constant,  $\gamma_e$ , for the expansion:  $B_v = B_e - \alpha_e (v + 1/2) + \gamma_e (v + 1/2)^2$

3. On-line NIST tables list  $\beta_e$  for the centrifugal distortion expansion:  $D_v = D_e + \beta_e (v + 1/2)$ .

#### Table Legend

H Data obtained from band head measurements (see Problem 3)

Z Data obtained from, or referring to, band origins (see Problem 3)

R Shaded towards longer wavelengths (appearance of the rotational fine-structure,  $B'_e < B''_e$ )

V Shaded towards shorter wavelengths (appearance of the rotational fine-structure,  $B'_e > B''_e$ )

( ) Uncertain data

[ ] Data refer to  $v = 0$  or lowest observed level.  $T_e$  values in square brackets give the energy of this level relative to the minimum of the ground-state potential energy curve. Vibrational frequencies in square brackets correspond to  $\Delta G(1/2)$  or the lowest observed interval.

*Answer:* The spectroscopic constants for the electronic term values,  $\tilde{T}_e$ , fundamental vibration frequencies,  $\omega_e = \tilde{\nu}_e$ , anharmonicities,  $\omega_e \chi_e = \chi_e \tilde{\nu}_e$ , and equilibrium bond lengths,  $r_e = R_e$ , are transcribed into cells D8:F11. The dissociation energy,  $\tilde{D}_e$ , and Morse  $a$ -parameter are calculated from the spectroscopic constants, Eqs. 27.5.6, 27.5.7, 27.5.12, and 27.5.17, allowing the potential energy curves to be calculated as columns in the spreadsheet.

Cell D13 for the dissociation energy of the ground state is: “=D12\*C4+D9/2-D10/4”

Cell E13 for the dissociation energy of the first excited state is: “=D\$13+\$C\$3-E8”

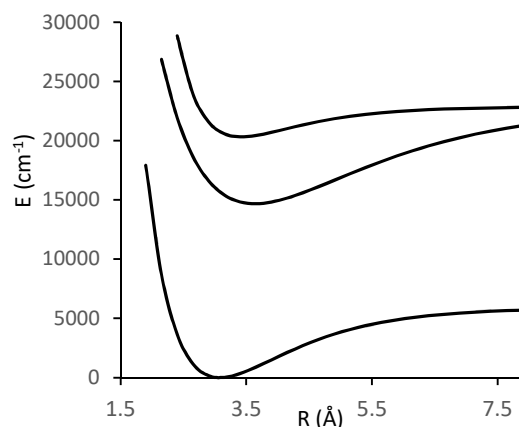
Cell D14 for the Morse  $a$ -parameter for the ground state is:

$$=2*PI()*D9*2.998E10*SQRT($C$2/1000/2/(D13*11.962))*1E-10$$

Cell D17 for the first cell of the Morse potential energy curve for the ground state is:

$$=D$8+D$13*(1-EXP(-D$14*($C17-D$11)))^2$$

A1	B	C	D	E	F	G
2	reduced mass	11.4949	g/mol			
3	$DE_{\text{atomic}} =$	16961	$\text{cm}^{-1}$			
4	1 eV =	8065.5	$\text{cm}^{-1}$			
5	1 $\text{cm}^{-1} =$	11.962	J/mol			
6						
7	State		X	A	B	
8	electronic	$T_e$	0	14680.6	20320.0	$\text{cm}^{-1}$
9	vib. freq.	$\nu_e$	159.125	117.323	124.09	$\text{cm}^{-1}$
10	anharmonic.	$\chi_e \nu_e$	0.7254	0.3576	0.6999	$\text{cm}^{-1}$
11	bond length	$R_e$	3.07887	3.6384	3.4228	$\text{\AA}$
12	dissoc. energy	$D_0$	0.720			eV
13	dissoc. energy	$D_e$	5886.54	8166.96	2527.52	$\text{cm}^{-1}$
14	Morse $a$	$a$	0.85636	0.53604	1.01915	
15	R step	0.25	$\text{\AA}$			
16		R ( $\text{\AA}$ )	V(X) $\text{cm}^{-1}$	V(A) $\text{cm}^{-1}$	V(B) $\text{cm}^{-1}$	
17		1.9	17910.6			
18		2.15	8695.89	26851.3		
19		2.4	3659.46	21931.2	28839.7	
20		2.65	1159.30	18666.8	23948.2	
21		2.9	161.29	16606.4	21571.7	
22		3.15	20.56	15412.0	20579.7	
23		3.4	340.28	14832.3	20321.4	
24		3.65	880.78	14680.9	20428.0	
25		3.9	1501.16	14820.4	20694.9	
26		4.15	2121.91	15150.4	21012.5	
27		4.4	2701.20	15598.1	21325.1	
28		4.65	3219.78	16111.4	21607.4	
29		4.9	3671.61	16653.4	21850.2	
30		5.15	4058.00	17198.6	22052.8	
31		5.4	4384.03	17729.9	22218.6	
32		5.65	4656.40	18236.3	22352.2	
33		5.9	4882.28	18710.9	22458.9	
34		6.15	5068.52	19150.5	22543.5	
35		6.4	5221.41	19553.5	22610.2	
36		6.65	5346.50	19920.2	22662.6	
37		6.9	5448.56	20251.9	22703.5	
38		7.15	5531.65	20550.3	22735.6	
39		7.4	5599.19	20817.7	22760.5	
40		7.65	5654.01	21056.4	22780.0	
41		7.9	5698.46	21268.9	22795.1	



Potential energy surfaces are the necessary starting point for molecular dynamics calculations of chemical kinetics rate constants.

38. The Huber-Herzberg tables of diatomic spectroscopic constants are introduced in the previous problem. Refer to the previous problem for interpretation and footnotes. (a) Find the  $^{12}\text{C}_2$  reference in the book or on-line, <http://webbook.nist.gov/chemistry>, and (b) write a spreadsheet to plot the potential energy surfaces as a function of  $R$  for the  $X^1\Sigma_g^+$  ground state, and  $a^3\Pi_u$ ,  $b^3\Sigma_g^-$ , and  $A^1\Pi_u$  excited states. Use the Morse function for the potential energy surfaces. The ground state dissociation energy is 6.21 eV. The  $a$  and  $b$  excited states dissociate to ground state atoms:  $\text{C}_2 \rightarrow \text{C}(^3\text{P}) + \text{C}(^3\text{P})$ . The  $A$  excited state dissociates to a ground state and an excited state atom:  $\text{C}_2 \rightarrow \text{C}(^3\text{P}) + \text{C}(^1\text{D})$ . The atomic excitation energy,  $\Delta E_{\text{atomic}}$ , is  $10192 \text{ cm}^{-1}$  to the  $^1\text{D}$  state. From Figure 28.2.5, note that  $\tilde{T}_e + \tilde{D}_e^{\text{ex}} = \tilde{D}_e + \Delta E_{\text{atomic}}$ .

*Answer:* The data table for  $C_2$  is reproduced below. The low lying  $a^3\Pi_u$  excited state is remarkable. Molecules don't typically have such low lying excited states.  $C_2$  is generated at high temperature is carbon arc sources and lightning strikes. At 2000 K, the occupancy of all excited  $^3\Pi$  states is roughly 82%.

State	$T_e$	$\omega_e$	$\omega_e\chi_e$	$\omega_e\nu_e$	$B_e$	$\alpha_e$	$D_e$	$r_e$	Trans.	$v_{00}$
$^{12}C_2$	$\mu = 6.000000$		$D_0^g = 6.21$ eV		$I.P. = 12.15$ eV					
F $^1\Pi_u$	[75456.9]	[1557.5] <sup>Z</sup>			1.645	0.019	6.E-6	1.307	F $\leftarrow$ X R	74532.9 <sup>Z</sup>
g $^3\Delta_g$	[73183.6]	[1458.06] <sup>Z</sup>			1.5238	0.17	6.60E-6	1.3579	g $\leftarrow$ a R	71649.6 <sup>Z</sup>
f $^3\Sigma_g^-$	71045.8	1360.5 <sup>Z</sup>	14.8		1.448	0.04	1.0E-5	1.393	f $\leftarrow$ a R	70188.4 <sup>Z</sup>
E $^1\Sigma_g^+$	55034.7	1671.50 <sup>Z</sup>	40.02	0.248	1.7897	0.0387	8.3E-6	1.2529	E $\rightarrow$ A V	46668.3 <sup>Z</sup>
d $^1\Sigma_u^+$	43239.44	1829.57 <sup>Z</sup>	13.94		1.8332	0.0196	7.32E-6	1.238	D $\leftrightarrow$ X	43226.74 <sup>Z</sup>
e $^3\Pi_g$	40796.65	1106.56 <sup>Z</sup>	39.26	2.805	1.1922	0.0242	6.3E-6	1.5351	e $\rightarrow$ a R	39806.46 <sup>Z</sup>
C $^1\Pi_g$	34261.3	1809.1 <sup>Z</sup>	15.81		1.7834	0.018	6.8E-6	1.2552	C $\rightarrow$ A VR	25969.19 <sup>Z</sup>
d $^3\Pi_g$	20022.5	1788.22 <sup>Z</sup>	16.44	-0.5067	1.7527	0.01608	6.74E-6	1.2661	d $\leftrightarrow$ a VR	19378.44 <sup>Z</sup>
c $^3\Sigma_u^+$	13312.1	1961.6	13.7		1.87			1.23		
A $^1\Pi_u$	8391	1608.35 <sup>Z</sup>	12.078	-0.01	1.6134	0.01686	6.44E-6	1.31843	A $\leftrightarrow$ X R	8268.16 <sup>Z</sup>
b $^3\Sigma_g^-$	6434.27	1470.45 <sup>Z</sup>	11.19	0.028	1.49852	0.01634	6.22E-6	1.36928	b $\rightarrow$ a R	5632.7 <sup>Z</sup>
a $^3\Pi_u$	716.24	1641.35 <sup>Z</sup>	11.67		1.63246	0.01661	6.44E-6	1.31190		
X $^1\Sigma_g^+$	0	1854.71 <sup>Z</sup>	13.340	-0.172	1.81984	0.01765	6.92E-6	1.24253		

The spreadsheet from the previous problem was used after adding an additional column. For the triplet a- and b-states,  $\Delta E_{\text{atomic}} = 0$  since the states dissociate to ground state C-atoms. The cells through the first half of the plot are reproduced below.

A1	B	C	D	E	F	G	H
2	reduced mass	11.49489	g/mol				
3	$\Delta E_{\text{atomic}} =$	10192	$\text{cm}^{-1}$				
4	1 eV =	8065.5	$\text{cm}^{-1}$				
5	1 $\text{cm}^{-1} =$	11.962	J/mol				
6							
7	State		X	a	b	A	
8	electronic term	$T_e$	0	716.24	6434.27	8391	$\text{cm}^{-1}$
9	vibration freq.	$\nu_e$	1854.71	1641.35	1470.45	1608.35	$\text{cm}^{-1}$
10	anharmonicity	$\chi_e\nu_e$	13.34	11.67	11.19	12.078	$\text{cm}^{-1}$
11	bond length	$R_e$	1.24253	1.3119	1.36928	1.31843	Å
12	dissoc. energy	$D_0$	6.210	6.21	6.21		eV
13	dissoc. energy	$D_e$	51010.775	50294.54	44576.51	52811.78	$\text{cm}^{-1}$
14	Morse $a$	$a$	3.3907203	3.021953	2.875704	2.889762	
15	R step	0.05	Å				
16		R (Å)	V(X) $\text{cm}^{-1}$	V(a) $\text{cm}^{-1}$	V(b) $\text{cm}^{-1}$	V(A) $\text{cm}^{-1}$	
17		1	83034.34				
18		1.05	43263.93	73938.33			
19		1.1	19696.11	41197.06	67374.14	49277.78	
20		1.15	6928.31	20747.87	40853.03	29151.20	
21		1.2	1227.49	8858.60	23964.17	17186.16	
22		1.25	31.91	2844.29	13897.95	10915.89	
23		1.3	1599.09	783.67	8600.83	8549.03	
24		1.35	4757.33	1311.11	6579.15	8792.50	
25		1.4	8730.70	3464.06	6752.95	10719.92	
26		1.45	13016.04	6571.32	8347.18	13673.90	
27		1.5	17296.81	10171.44	10810.80	17193.63	
28		1.55	21382.86	13953.10	13756.75	20961.25	
29		1.6	25168.59	17711.84	16917.42	24762.37	
30		1.65	28603.94	21318.53	20111.80	28456.87	
31		1.7	31674.56	24696.67	23221.15	31957.50	

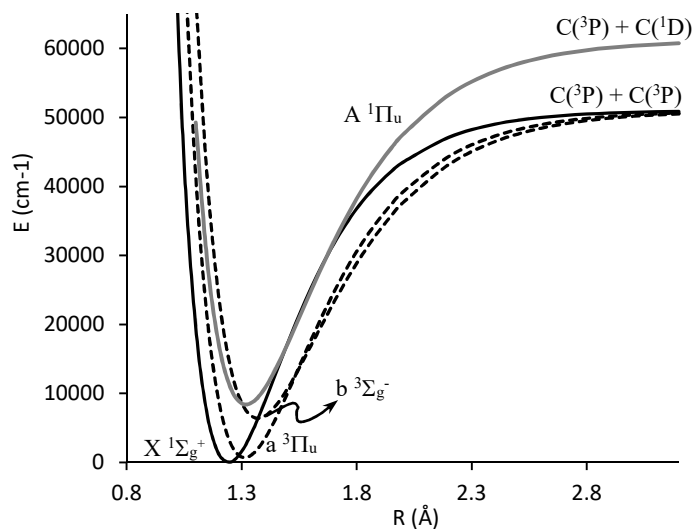


Figure P28.38.1: Potential energy surfaces for the four lowest electronic states of  $C_2$ . The singlet states are shown as solid lines and the triplet states are shown as dotted.

$C_2$  is the source of blue light from flames and the glow from some comets.<sup>1</sup> Synthesis with reactive carbon species is an established area in organic chemistry. The reactive carbon species are typically generated in high current carbon arc discharges.<sup>11</sup>  $C_2$  undoubtedly plays a role in some of these systems. The relevance of this work extends to the formation of organic compounds in interstellar space and in pre-biotic environments in lightning strikes.

39. In Chapter 27, we did not justify the vibrational selection rule that in absorption, the transition dipole moment vanishes unless the normal mode transforms according to the same representation as the x, y, or z-component of the electric dipole moment. The transition electric dipole moment is proportional to the integral given by Eqs. 27.9.13. For a diatomic molecule aligned along the x-axis, the harmonic oscillator wave functions are functions of the displacement along the x-axis,  $x = R - R_0$ . The electric dipole operator along the internuclear axis is also a function of the x-axis position of the nuclei and the partial charge on the atoms. The transition dipole moment is then proportional to:

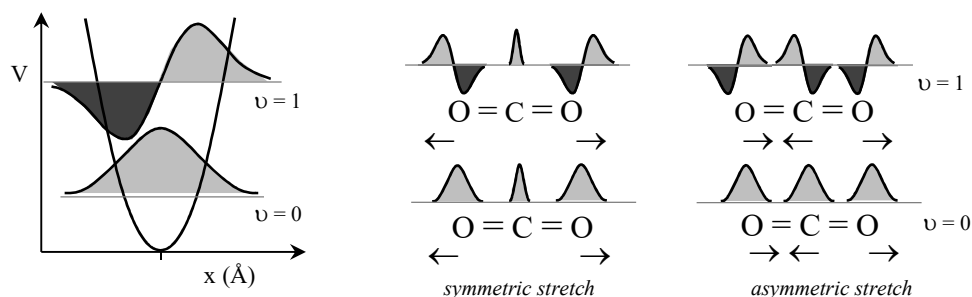
$$\mu_{tr,x} \propto \int_{-\infty}^{\infty} \chi_{v'} x \chi_{v''} dx$$

The integrand contains three functions, the final harmonic oscillator wave function with quantum number  $v'$ , the x-operator, and the initial harmonic oscillator wave function with quantum number  $v''$ . The x-operator is purely odd. The integral is over all space, so that the integral vanishes for an odd integrand. As a consequence the product of the three functions must be overall even for the transition moment integral to be non-zero.

For polyatomics, we must consider the x, y, and z-components of the transition dipole. The symmetry of each vibrational wave function is represented by an irreducible representation of the point group of the molecule. Consider the case for the fundamental transition  $1 \leftarrow 0$ . The ground

state vibrational wave function,  $\nu = 0$ , always transforms according to the totally symmetric irreducible representation. As a result, to give a non-vanishing integral the product of the excited state vibrational wave function and the  $x$ -operator must contain the totally symmetric irreducible representation. The normal mode must transform according to the same representation as the  $x$ ,  $y$ , or  $z$ -component of the electric dipole moment.

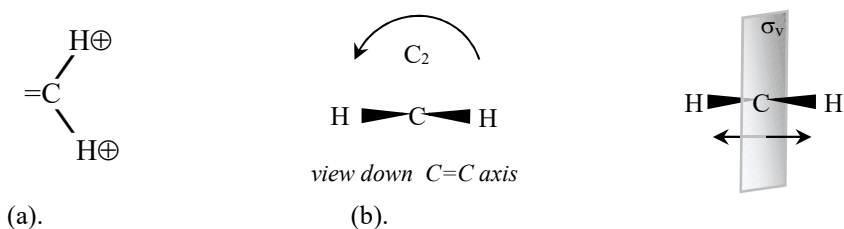
How can we illustrate that the ground vibrational state is totally symmetric under the operations of the point group? Consider a simple polyatomic such as  $\text{CO}_2$  as compared to a diatomic molecule. The diatomic harmonic oscillator wave functions for  $\nu = 0$  and 1 are shown at left and the corresponding wave functions are illustrated for  $\text{CO}_2$  at right, Figure P28.39.1. The ground state,  $\nu = 0$ , wave function of any normal mode necessarily retains the same sign upon any symmetry operation of the point group, since the wave function is always positive. Now, consider the action of the reflection operator on the excited state wave function. For the  $\nu = 1$  state, the inversion operation is symmetric for the symmetric stretch and anti-symmetric for the asymmetric stretch. As a result, the symmetric stretch is IR-inactive and the asymmetric stretch is IR-active.



(a). Diatomic vibrational wave functions      (b). Polyatomic normal modes

Figure 28.39.1: Symmetry of harmonic oscillator wave functions for (a) diatomics and (b) the symmetric and asymmetric stretch of  $\text{CO}_2$ . The  $\text{CO}_2$  symmetric stretch is symmetric with respect to a plane perpendicular to the internuclear axis, passing through the center of mass (a  $\sigma_v$ -plane). The asymmetric stretch is anti-symmetric with respect to reflection.

The symmetry of bending vibrations is possibly confusing, based on displacement arrows. Please review Problem 27.38. For this problem, using depictions of the quantum mechanical wave function of the type shown in Figure 28.39.1b, determine the symmetry of the wag-bending vibration with respect to  $C_2$ -rotation and reflection across  $\sigma_v$ , Figure 28.39.2:



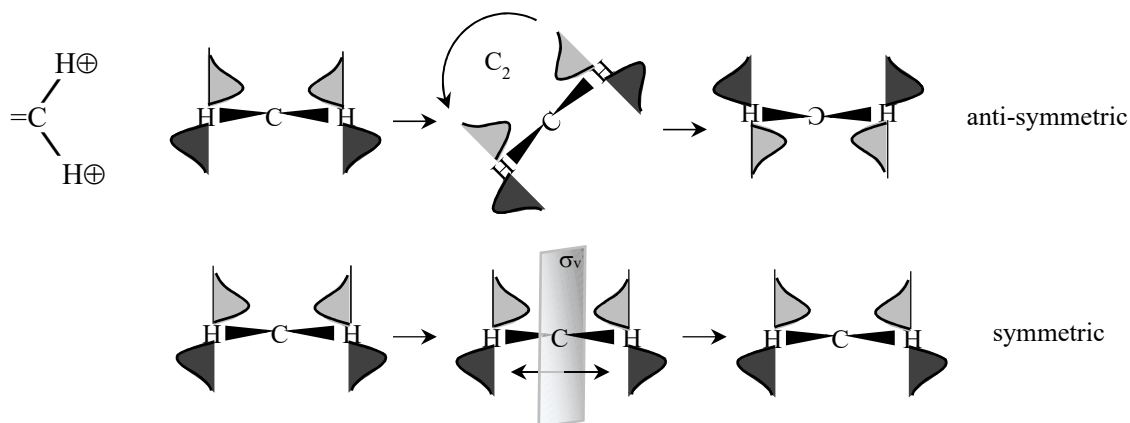
(a).

(b).

Figure 28.39.2: (a). Top down view of the wag-mode of a  $\text{CH}_2$  group. (b). End-on view, down the  $\text{C}=\text{C}$  internuclear axis, showing the  $C_2$ -rotation and  $\sigma_v$ -reflection operations.

*Answer:* The plan is to note that the wag-bending vibration will have in-phase “blobs” of probability above and below the plane of the equilibrium atom positions.

A schematic depiction of the harmonic oscillator wave function that roughly applies to a bending vibration is shown below. The phase of the lobes is that the positive lobe is in the positive direction for motion of both H-atoms.  $C_2$ -rotation inverts the sign of the wave function while reflection maintains the phase of the wave function. The wag transforms as the  $B_1$  irreducible representation of the  $C_{2v}$ -point group, for example. The rock, which is the other bending vibration depicted in Problem 27.38, transforms as  $B_2$  under  $C_{2v}$ .



### Literature Cited:

1. R. Hoffmann, "C<sub>2</sub> In All Its Guises," *American Scientist*, **1995**, 83, 309–311.
2. K. P. Huber and G. Herzberg, *Constants of diatomic molecules*, (data prepared by J. W. Gallagher and R. D. Johnson, III) in NIST Chemistry WebBook, NIST Standard Reference Database Number 69, Eds. P. J. Linstrom and W. G. Mallard, National Institute of Standards and Technology, Gaithersburg MD, <http://webbook.nist.gov/chemistry>, (last accessed 4/2015).
3. K. P. Huber and G. Herzberg, *Molecular Spectra and Molecular Structure: IV. Constants of diatomic molecules*, Van Nostrand Reinhold, New York, NY, 1979.
4. G. Herzberg, *Molecular Spectra and Molecular Structure: Spectra of Diatomic Molecules*, 2<sup>nd</sup>. Ed., Van Nostrand Reinhold, New York, NY, 1950. pp. 212-216, 240-243.
5. A. G. Gaydon, *Dissociation Energies and Spectra of Diatomic Molecules*, Dover, New York, NY, 1950.
6. E. E. Vago, R. F. Barrow, "Ultra-violet Absorption Band-Systems of SiS, SiSe, and SiTe," *Proc. Phys. Soc.*, **1946**, 58, 538-544.
7. H. J. Lempka, T. R. Passmore, W. C. Price, "The photoelectron spectra and ionized states of the halogen acids," *Proc. Roy. Soc. A.*, **1968**, 304, 53-64. Spectrum simulated from numerical data.
8. D. W. Turner, "Molecular photoelectron spectroscopy," *Phil. Trans. Roy. Soc. Lond. A.*, **1970**, 268, 7-31.
9. M. S. Lojko, Y. Beers, "A Table of Rotational Constants of Symmetric Top Molecules Giving Rise to Microwave Spectra," *J. Research National Bureau of Standards – A. Physics and Chemistry*, **1969**, 73A(2), 233-239. Available online at (last accessed 4/8/2015):

[http://nvlpubs.nist.gov/nistpubs/jres/73A/jresv73An2p233\\_A1b.pdf](http://nvlpubs.nist.gov/nistpubs/jres/73A/jresv73An2p233_A1b.pdf)

10. D. C. Harris, M. D. Bertolucci, *Symmetry and Spectroscopy: An Introduction to Vibrational and Electronic Spectroscopy*, Oxford, New York, NY, 1978. pp. 372-373.
11. P. B. Shevlin, "Atomic Carbon," in *Reactive Intermediate Chemistry*; R. A. Moss, M. S. Platz, M. Jones, Jr., Eds., Wiley-Interscience, Hoboken, NJ, 2004. Chapter 10.